

Accepted Manuscript



The Bile Acid Receptor TGR5 Activates the TRPA1 Channel to Induce Itch in Mice

TinaMarie Lieu, Gihan Jayaweera, Peishen Zhao, Daniel P. Poole, Dane Jensen, Megan Grace, Peter McIntyre, Romke Bron, Yvette M. Wilson, Matheus Krappitz, Silke Haerteis, Christoph Korbmayer, Martin S. Steinhoff, Romina Nassini, Serena Materazzi, Pierangelo Geppetti, Carlos U. Corvera, Nigel W. Bunnett

PII: S0016-5085(14)01081-6
DOI: [10.1053/j.gastro.2014.08.042](https://doi.org/10.1053/j.gastro.2014.08.042)
Reference: YGAST 59325

To appear in: *Gastroenterology*
Accepted Date: 26 August 2014

Please cite this article as: Lieu T, Jayaweera G, Zhao P, Poole DP, Jensen D, Grace M, McIntyre P, Bron R, Wilson YM, Krappitz M, Haerteis S, Korbmayer C, Steinhoff MS, Nassini R, Materazzi S, Geppetti P, Corvera CU, Bunnett NW, The Bile Acid Receptor TGR5 Activates the TRPA1 Channel to Induce Itch in Mice, *Gastroenterology* (2014), doi: 10.1053/j.gastro.2014.08.042.

This is a PDF file of an unedited manuscript that has been accepted for publication. As a service to our customers we are providing this early version of the manuscript. The manuscript will undergo copyediting, typesetting, and review of the resulting proof before it is published in its final form. Please note that during the production process errors may be discovered which could affect the content, and all legal disclaimers that apply to the journal pertain.

All studies published in *Gastroenterology* are embargoed until 3PM ET of the day they are published as corrected proofs on-line. Studies cannot be publicized as accepted manuscripts or uncorrected proofs.

The Bile Acid Receptor TGR5 Activates the TRPA1 Channel to Induce Itch in Mice**Short Title:** Bile Acid Evoked Itch

TinaMarie Lieu¹, Gihan Jayaweera¹, Peishen Zhao¹, Daniel P. Poole^{1,3}, Dane Jensen¹, Megan Grace², Peter McIntyre², Romke Bron³, Yvette M. Wilson³, Matteus Krappitz⁴, Silke Haerteis⁴, Christoph Korbmacher⁴, Martin S. Steinhoff⁵, Romina Nassini⁶, Serena Materazzi⁶, Pierangelo Geppetti⁶, Carlos U. Corvera⁷, Nigel W. Bunnett^{1,8}

¹Monash Institute of Pharmaceutical Sciences, Parkville, Victoria 3052, Australia; ²Health Innovations Research Institute and School of Medical Sciences, RMIT University, Bundoora, Victoria 3083, Australia; Departments of ³Anatomy and Neuroscience and ⁸Pharmacology, University of Melbourne, Parkville, Victoria 3010, Australia; ⁴Institut für Zelluläre und Molekulare Physiologie, Friedrich-Alexander-Universität Erlangen-Nürnberg, D-91054, Erlangen, Germany; ⁵Charles Institute for Translational Dermatology, University College Dublin, Dublin-4, Ireland; ⁶Department of Health Sciences, Clinical Pharmacology Unit, University of Florence, 6-50139, Florence, Italy; ⁷Department of Surgery, University of California, San Francisco, San Francisco, CA 94131, USA.

Grant Support and Acknowledgements: Supported by NHMRC 63303, 1049682, 1031886 and Monash University (N.W.B.). We thank Tao Yu and Cameron Nowell for technical assistance.

Abbreviations: AITC, allyl isothiocyanate; BA, bile acid; DiI, Diiododecyl-3,3',3'-Tetramethylindocarbocyanine Perchlorate; DCA, deoxycholic acid; DRG, dorsal root ganglia; GRP, gastrin-releasing peptide; IR, immunoreactivity; NPPB, natriuretic polypeptide B; TLCA, tauroolithocholic acid; TRPA1, transient receptor potential ankyrin 1.

Correspondence: Nigel Bunnett, B.Sc., Ph.D., Monash Institute of Pharmaceutical Sciences, 381 Royal Parade, Parkville, VIC 3052, Australia. Tel: Office - +61 3 9903 9136; Mobile - +61 407 392 619. Facsimile: +61 3 9903 9581. Email: Nigel.Bunnett@Monash.edu

Disclosures: The authors declare no conflict of interest.

Author contributions: TL, GJ, PZ, DPP, DJ, MG, RB, YMW, MK, SH, RN, SM: generation of data; PM, CK, MSS, PG, CUC, NWB: conception of study; NWB, MSS: writing manuscript.

Abstract

Background & Aims: Patients with cholestatic disease have increased systemic concentrations of bile acids (BAs) and profound pruritus. The G protein-coupled BA receptor 1 TGR5 (encoded by *GPBAR1*) is expressed by primary sensory neurons; its activation induces neuronal hyperexcitability and scratching, by unknown mechanisms. We investigated whether the transient receptor potential ankyrin 1 (TRPA1) is involved in BA-evoked, TGR5-dependent pruritus in mice.

Methods: Co-expression of TGR5 and TRPA1 in cutaneous afferent neurons isolated from mice was analyzed by immunofluorescence, in situ hybridization, and single-cell PCR. TGR5-induced activation of TRPA1 was studied in HEK293 cells, *Xenopus laevis* oocytes, and primary sensory neurons by measuring Ca^{2+} signals. The contribution of TRPA1 to TGR5-induced release of pruritogenic neuropeptides, activation of spinal neurons, and scratching behavior were studied using TRPA1 antagonists or *Trpa1*^{-/-} mice.

Results: TGR5 and TRPA1 protein and mRNA were expressed by cutaneous afferent neurons. In HEK cells, oocytes, and neurons co-expressing TGR5 and TRPA1, BAs caused TGR5-dependent activation and sensitization of TRPA1 by mechanisms that required $G\beta\gamma$, protein kinase C and Ca^{2+} . Antagonists or deletion of TRPA1 prevented BA-stimulated release of the pruritogenic neuropeptides gastrin-releasing peptide and atrial natriuretic peptide B in the spinal cord. Disruption of *Trpa1* in mice blocked BA-induced expression of Fos in spinal neurons and prevented BA-stimulated scratching. Spontaneous scratching was exacerbated in transgenic mice that overexpressed TRG5. Administration of a TRPA1 antagonist or the BA sequestrant colestipol, which lowered circulating levels of BAs, prevented exacerbated spontaneous scratching in TGR5 overexpressing mice.

Conclusions: BAs induce pruritus in mice by co-activation of TGR5 and TRPA1. Antagonists of TGR5 and TRPA1, or inhibitors of the signaling mechanism by which TGR5 activates TRPA1, might be developed for treatment of cholestatic pruritus.

KEYWORDS: liver, mouse model, itching, signal transduction

Introduction

Itch induces the protective reflex of scratching that removes irritants and parasites from the skin. However, chronic itch that is associated with disease (*e.g.*, hepatic, renal, neurological disorders, eczema, certain cancers) is debilitating, poorly understood and difficult to treat ¹. A deeper understanding of the mechanisms of disease-associated itch is required to develop more effective therapies.

Pruritogens induce itch by activating G protein-coupled receptors (GPCRs) and transient receptor potential (TRP) ion channels on cutaneous afferent nerve endings. Histamine from mast cells activates the histamine H₁ receptor that, *via* phospholipase-C (PLC) signaling, sensitizes TRP vanilloid 1 (TRPV1), which is necessary for neuronal excitation and scratching ². Although antagonists of the H₁ receptor are useful therapies for this acute allergic itch, anti-histamines are ineffective for chronic itch. Pruritogens that induce histamine-independent itch include the anti-malarial drug chloroquine, which activates the Mas-related GPCR MrgprA3, the endogenous peptide pruritogen BAM8-22, which activates MrgprC11 ³, and proteases that activate protease-activated receptor-2 ⁴. MrgprA3 and MrgprC11 respectively activate Gβγ and PLC signaling pathways that sensitize TRP ankyrin 1 (TRPA1), which is required for the acute excitatory and pruritogenic actions of chloroquine and BAM8-22 ⁵. TRPA1 is also necessary for the exacerbated scratching of mice with dry skin ⁶. However, the contribution of TRPA1 to acute and chronic itch that is induced by disease-relevant endogenous pruritogens has not been studied, and the contribution of TRPA1 to the release of neuropeptides that transmit itch, including gastrin-releasing peptide (GRP) ⁷ and natriuretic polypeptide B (NPPB) ⁸, is unknown.

We recently identified the bile acid (BA) GPCR TGR5 as a major mediator of BA-evoked scratching in mice ⁹. Patients with cholestatic liver disease, which is characterized by deficient bile secretion into the intestine, can develop chronic pruritus that is so severe and intractable that it is an indication for liver transplantation ¹⁰. BAs may cause cholestatic pruritus since BA levels are increased in the circulation ¹¹ and skin ¹² of patients with cholestasis, BA chelators relieve cholestatic pruritus ¹³, and application of BAs to the skin causes itch ¹⁴. TGR5 is expressed by primary afferent neurons, and BAs induce neuronal excitability, stimulate release of GRP in the spinal cord, and evoke scratching by TGR5-dependent mechanisms ⁹. The role of TRPA1 in BA-evoked itch is unexplored.

Herein we report a major role for TGR5-dependent activation of TRPA1 in the pruritogenic actions of exogenous BAs, and define the importance of this pathway for the actions of a disease-relevant endogenous pruritogen.

Materials and Methods

See Supplemental Material for sources of animals and materials, and for detailed methods.

Animals. Institutional Animal Ethics Committees approved all studies.

Retrograde tracing. 1,1'-Dioctadecyl-3,3,3',3'-Tetramethylindocarbocyanine Perchlorate (DiI, 2%, 10 μ l, intradermal) was injected to the nape of the neck and mice were recovered for 7 days.

Immunofluorescence, in-situ hybridization. Dorsal root ganglia (DRG, C1-C7) were fixed, sectioned and processed to detect TGR5, NeuN and HuC/D by indirect immunofluorescence⁹ and TRPA1 by *in situ* hybridization¹⁵.

Single cell RT-PCR. DRG were dissociated and individual DiI-positive small diameter (<25 μ m) neurons were aspirated⁹. PCR reactions used intron-spanning mouse primers for TGR5, TRPA1, TRPV1, or β -actin.

Cell lines. HEK293 cells stably expressing human TGR5 have been described¹⁶. HEK293 cells expressing human TRPA1 alone or together with TGR5 were generated using a tetracycline-inducible system.

[Ca²⁺]_i assays in HEK cells. HEK cells were loaded with Fura-2/AM, and fluorescence of populations of cells was measured (340/380 nm excitation, 530 nm emission). Cells were challenged with DCA (100 μ M, 5 min) and then allyl isothiocyanate (AITC, 100 μ M, 5 min). Cells were incubated with H89 (10 μ M, protein kinase A, PKA inhibitor), GF109203X (10 μ M, protein kinase C, PKC inhibitor), gallein (100 μ M, G β γ inhibitor), HC-030031 (100 μ M, TRPA1 antagonist), or vehicle (control) (60 min preincubation and inclusion throughout).

Isolation and culture of DRG neurons. DRG from all spinal levels were dissociated and maintained for 24 h before assays⁹.

[Ca²⁺]_i assays in DRG neurons. Neurons were loaded with Fura-2/AM and fluorescence of individual small diameter neurons (<25 μ m) was measured (340/380 nm excitation, 530 nm emission). Neurons were challenged sequentially with AITC (100 μ M), DCA (100 μ M), capsaicin (1 μ M), and KCl (50 mM). Neurons were incubated with GF109203X (10 μ M), gallein (100 μ M), HC-030031 (100 μ M) or vehicle (control) (30 or 60 min preincubation and inclusion throughout), or were assayed in Ca²⁺-free buffer containing 2 mM EDTA.

ERK1/2 activation in DRG neurons. Neurons were serum-starved for 6 h, challenged with DCA (100 μ M) or phorbol 12,13-dibutyrate (PDBu, 200 nM, positive control) for 30 min at 37°C, and lysed. ERK1/2 activation was assessed using AlphaScreen phospho-ERK assay.

cAMP accumulation in DRG neurons. Neurons were serum-starved for 6 h, incubated in activation buffer (DMEM, 5 mM HEPES, 0.1% BSA, 1 mM 3-isobutyl-1-methylxanthine) for 45 min, challenged with DCA (100 μ M) or forskolin (10 μ M, positive control) for 30 min at 37°C, and lysed. cAMP accumulation was assessed using AlphaScreen cAMP assay.

TRPA1 currents in *Xenopus laevis* oocytes. Oocytes were injected with cRNA encoding human TRPA1 alone (0.5 ng) or both TRPA1 (0.5 ng) plus humanTGR5 (2 ng). Oocytes were studied after 2 days by

two-electrode voltage-clamp¹⁷. AITC (50 μ M) and HC-030031 (15 μ M) were used to activate and inhibit TRPA1 currents, respectively. DCA (500 μ M) was used to activate TGR5.

Neuropeptide release. Slices of rat spinal cord with attached dorsal roots (combined cervical, thoracic, lumbar-sacral segments) were prepared and superfused with Krebs solution⁹. Slices were stimulated with TLCA (500 μ M), AITC (100 μ M) or vehicle for 60 min. Some tissues were superfused with HC-030031 (50 μ M) or vehicle wiping behavior. for 20 min before and during the stimulus. GRP and NPPB release were determined by enzyme immunoassays, and peptide concentrations were calculated as fmol.g⁻¹ tissue wet weight.

c-fos in spinal neurons. Mice were sedated (isoflurane) and DCA (25 μ g, 10 μ l, s.c.) or vehicle (0.9% NaCl) was injected into the nape of the neck. They were either allowed to recover from sedation or were kept sedated to exclude scratching-induced activation of spinal neurons. Some groups were pretreated with HC-030031 (100 mg.kg⁻¹ p.o.) or vehicle (100 μ l) 30 min before DCA. At 60 min after DCA, mice were anesthetized and transcardially fixed. Frozen sections of cervical spinal cord were made and processed to detect β -galactosidase¹⁸. β -galactosidase (*c-fos*) -positive cells in dorsal horn laminae I-III were counted by an observer unaware of the treatment.

Scratching and nociception. Behavior was assessed in mice by an investigator unaware of treatment groups^{9,19}. Mice were sedated (isoflurane) and DCA (25 μ g, 10 μ l, s.c.) was injected into the nape of the neck. Some groups were pretreated with HC-030031 (100 mg.kg⁻¹, p.o., in 2% DMSO, 20% cyclodextrin), AMG-9810 (40 mg.kg⁻¹, i.p., in 0.9% saline) or vehicle (100 μ l) 30 min before DCA injection. Scratching behavior was recorded ~2 h after food withdrawal for 60 min after DCA injection⁹. The effectiveness of AMG-9810 as a TRPV1 antagonist was determined by its capacity to suppress pain-related wiping behavior in response to capsaicin (3 μ g, 10 μ l, s.c.) into the cheek¹⁹.

BA sequestrant. *Tgr5-tg* mice were treated with the BA sequestrant colestipol hydrochloride (2.5 mg.kg⁻¹, p.o.) or vehicle (0.9% NaCl, p.o.) at 08:00 and 14:00 h for 5 days. After the final dose spontaneous scratching behavior was recorded for 60 min. Some mice received HC-030031 (100 mg.kg⁻¹) or vehicle 30 min before scratching behavior was recorded.

Plasma BAs. *Tgr5-tg* mice treated with colestipol or vehicle were killed at the end of the scratching assays. Blood was collected at ~4 h after food withdrawal by cardiac puncture for assay of total plasma BAs.

Statistics. Results are expressed as mean \pm SEM. Data were compared statistically using a Student's t-test (2 groups) or ANOVA and Bonferroni or Tukey-Kramer *post hoc* test (multiple groups). $P < 0.05$ was considered significant.

Results

TGR5 is co-expressed with TRPA1 in a population of primary afferent neurons that innervate the skin.

To identify dorsal root ganglia (DRG) neurons that innervate the skin, we injected the retrograde tracer DiI intradermally (nape of neck) in mice. TGR5 was detected using an antibody that specifically detects TGR5 in small diameter neurons of wild-type but not *tgr5*^{-/-} mice⁹. TGR5 and the pan-neuronal markers NeuN or Hu-C/D were localized by immunofluorescence, and TRPA1 was detected by *in situ* hybridization. All DiI-containing cells expressed NeuN immunoreactivity (IR) or Hu-C/D-IR, and are thus neurons (Fig. 1). TGR5-IR was detected in a sub-population of small diameter (<25 μ m) neurons that contained DiI, although some DiI-containing neurons did not express TGR5-IR (Fig. 1A, B). Of the DiI-containing neurons, 18.2 \pm 2.4% expressed TGR5-IR and 81.8 \pm 2.4% did not express detectable TGR5 (889 neurons, n=6 mice) (Fig. 1B). TGR5-IR and TRPA1 mRNA were colocalized in a proportion of DiI-containing neurons (Fig. 1C). TRPA1 mRNA was detected in 20.5 \pm 1.4% and TGR5-IR and TRPA1 mRNA were co-expressed in 4.2 \pm 0.4% of all DRG neurons (1850 neurons, n=6 mice) (Fig. 1D). TRPA1 mRNA was detected in 28.3 \pm 3.2% and TGR5-IR and TRPA1 mRNA were co-expressed in 7.0 \pm 0.7% of cutaneous afferent neurons (Fig. 1D). By using single cell RT-PCR, we detected transcripts corresponding to TGR5 (236 bp), TRPA1 (393 bp) and TRPV1 (229 bp) in DiI-containing neurons (Fig. 1E). Analysis of 60 small diameter DiI-containing neurons from 6 mice revealed that 37% (22/60) expressed TRPV1, 20% (12/60) expressed TRPA1, and 8% (5/60) expressed TGR5 (Fig. 1F). All TGR5-positive neurons (5/5) co-expressed TRPA1.

TGR5 activates and sensitizes TRPA1 in HEK293 cells by a G $\beta\gamma$ and protein kinase C-mediated mechanism. To examine the functional interactions between TGR5 and TRPA1, we expressed in HEK293 cells TGR5 and TRPA1 separately or together. We assessed TRPA1 activation by measuring [Ca²⁺]_i. Cells were challenged with vehicle or deoxycholic acid (DCA, 100 μ M), a TGR5 agonist, and 5 min later were stimulated with the TRPA1 agonist AITC (100 μ M). In HEK-TGR5 cells, vehicle, DCA or AITC did not affect [Ca²⁺]_i (Fig. 2A, E, F). In contrast, in HEK-TGR5+TRPA1 cells, DCA but not vehicle induced a prompt increase in [Ca²⁺]_i (Fig. 2A, E). The response of HEK-TGR5+TRPA1 cells to AITC was larger in cells pretreated with DCA when compared to vehicle (Fig. 2A, F). The observation that DCA increases [Ca²⁺]_i in HEK-TGR5+TRPA1 but not in HEK-TGR5 cells indicates that TGR5 can activate TRPA1 to induce an influx of extracellular Ca²⁺ ions. In support of this proposal, DCA-evoked increases in [Ca²⁺]_i in HEK-TGR5+TRPA1 cells were abolished by the TRPA1 antagonist HC-030031 (100 μ M) (Fig. 2D, F). The finding that DCA-pretreatment amplified the response of HEK-TGR5+TRPA1 cells to AITC suggests that activation of TGR5 by DCA can also sensitize TRPA1. DCA did not increase [Ca²⁺]_i in HEK-TRPA1 cells, indicating that DCA cannot directly activate TRPA1 (not shown).

GPCRs activate and sensitize TRP channels *via* G α and G $\beta\gamma$ signaling. G $\beta\gamma$ subunits can directly open certain channels²⁰, and G $\beta\gamma$ mediates MrgprA3-evoked activation of TRPA1⁵. G α can activate PKA and PKC, which phosphorylate and activate TRP channels²¹. The G $\beta\gamma$ inhibitor gallein (100 μ M) and the

PKC inhibitor GF109203X (10 μ M) inhibited DCA-evoked increases in $[Ca^{2+}]_i$ in HEK-TGR5+TRPA1 cells (Fig. 2B, C, E). In contrast, gallein and GF109203X did not prevent DCA-induced sensitization of the response to AITC (Fig. 2B, C, F). Thus, $G\beta\gamma$ and PKC are required for TGR5-induced activation but not sensitization of TRPA1. The PKA inhibitor H89 (10 μ M) amplified DCA-evoked increases in $[Ca^{2+}]_i$ in HEK-TGR5+TRPA1 cells without affecting DCA-induced sensitization of the response to AITC (Fig. 2D, E, F). PKA may desensitize TGR5, which couples to cAMP and PKA²².

TGR5 stimulates TRPA1 currents in *Xenopus laevis* oocytes. In oocytes expressing TRPA1 alone or TRPA1 and TGR5, AITC (50 μ M) elicited a transient inward current that was prevented or reversed by HC-030031 (15 μ M) consistent with activation of TRPA1 (Fig. 3A, B). To determine whether activation of TGR5 sensitizes TRPA1 currents, oocytes co-expressing TRPA1 and TGR5 were exposed to DCA (500 μ M) or vehicle (control) for 30 s prior to AITC. Pre-incubation with DCA resulted in a ~40% increase of the AITC-evoked TRPA1 current compared to vehicle-treated oocytes (Fig. 3C). In contrast, DCA did not increase the AITC current response in oocytes expressing TRPA1 alone. Thus, the stimulatory effect of DCA on TRPA1 currents requires co-expression of TGR5, and DCA does not directly activate TRPA1. Chelation of intracellular Ca^{2+} ions using BAPTA-AM (100 μ M) prevented DCA-evoked sensitization of TRPA1, which is Ca^{2+} -dependent (Fig. 3D). BAPTA-AM increased the baseline AITC response by unknown mechanisms.

TGR5 activates TRPA1 in primary afferent neurons by a $G\beta\gamma$ and PKC-mediated mechanism. DCA (100 μ M) stimulated generation of cAMP and activation of ERK1/2 in DRG neurons isolated from wild-type but not *tgr5*^{-/-} mice (Supplemental Fig. 1A, B), which indicates that DCA signals to DRG neurons by a TGR5-dependent process. To assess the interactions between TGR5 and TRP channels in DRG neurons, we measured $[Ca^{2+}]_i$ in individual neurons, and determined the magnitude of responses and the proportions of responsive neurons. Neurons were sequentially challenged with the TRPA1 agonist AITC (100 μ M), the TGR5 agonists DCA or tauro lithocholic acid (TLCA) (100 μ M), the TRPV1 agonist capsaicin (1 μ M), and finally with KCl (50 mM). In wild-type mice, AITC, DCA and capsaicin all caused a robust increase in $[Ca^{2+}]_i$ in a subpopulation of neurons (Fig. 4A). Of all small diameter KCl-responsive neurons, 27.1 \pm 5.6% responded to DCA and 32.8 \pm 7.8% responded to TLCA (1435 neurons from 12 mice, 846 neurons from 5 mice, respectively) (Fig. 4F). Removal of extracellular Ca^{2+} ions prevented AITC-, DCA- and capsaicin-induced increases in $[Ca^{2+}]_i$ (Fig. 4B, F). The responses to AITC and capsaicin were retained in neurons from *tgr5*^{-/-} mice, whereas TGR5 deletion abolished the response to DCA (Fig. 4C, F; Supplemental Fig. 2A). In neurons from *trpa1*^{-/-} mice, the responses to both AITC and DCA were absent, whereas the response to capsaicin was retained (Fig. 4D, F; Supplemental Fig. 2A). In wild-type mice, the TRPA1 antagonist HC-030031 similarly prevented DCA- and AITC- but not capsaicin-evoked increases in $[Ca^{2+}]_i$ (Fig. 4E, F). The $G\beta\gamma$ inhibitor gallein and the PKC inhibitor GF109203X both prevented DCA-

evoked increases in $[Ca^{2+}]_i$ in neurons from wild-type mice (Fig. 4F, Supplemental Fig. 2B, C). GF109203X, but not gallein, also inhibited the AITC response in neurons, but neither affected to capsaicin response. In neurons from *trpv1*^{-/-} mice, the responses to AITC and DCA were preserved, whereas the response to capsaicin was absent (Fig. 4F; Supplemental Fig. 2D). *Trpv1* deletion reduced the proportion of DCA-responsive neurons, but the change was not significant.

In wild-type mice, 33.3±6.2% of AITC-responsive neurons also responded to DCA. Moreover, 27.1±5.6% of wild-type neurons responded to AITC, DCA and capsaicin, whereas 6.2±2.1% of neurons responded to AITC and DCA but not capsaicin (Fig. 5A). Removal of extracellular Ca^{2+} ions suppressed responses to AITC, DCA and capsaicin (Fig. 5B). Deletion of TGR5 and deletion or antagonism of TRPA1 abolished responses to DCA (Fig. 5C, D, E). TRPA1 deletion and antagonism also blocked responses to AITC (Fig. 5D, E). In wild-type mice, 32.8±7.8% of neurons responded to AITC, TLCA and capsaicin, whereas 6.8±1.4% of neurons responded to AITC and TLCA but not capsaicin (Fig. 5F).

Thus, DCA and TLCA stimulate TGR5, which activates TRPA1 *via* Gβγ and PKC to promote the influx of extracellular Ca^{2+} ions in small diameter DRG neurons of mice.

BAs induce TRPA1-dependent release of the itch transmitters GRP and NPPB. Pruritogens stimulate release of the itch-selective transmitters GRP and NPBB in the dorsal horn of the spinal cord by unknown mechanisms^{7,8}. To study neuropeptide release, we superfused slices of rat dorsal spinal cord with vehicle or the TGR5 agonist TLCA (500 μM, 60 min) and measured release of GRP and NPPB by ELISA. Rats provided an adequate amount of tissue to reproducibly measure peptide release, and tissues were stimulated with TLCA, which is a more potent TGR5 agonist and stimulant of neuropeptide release than DCA^{9, 23, 24}. In vehicle-treated tissues, TLCA stimulated a 6.4-fold release of GRP-immunoreactivity (GRP-IR) and a 5.3-fold release of NPPB-IR over baseline (Fig. 6A, B). The TRPA1 agonist AITC (100 μM, 60 min) stimulated release of calcitonin gene-related peptide (CGRP)-IR, GRP-IR and NPPB-IR (Supplemental Fig. 3A-C). HC-030031 (50 μM) abolished TLCA- and AITC-stimulated neuropeptide release. Thus, TRPA1 activity is necessary for BA-evoked release of pruritogenic peptides in the spinal cord.

BAs activate spinal neurons by a TRPA1-dependent mechanism. To determine whether cutaneous BAs pruritogens activate spinal neurons, we studied transgenic mice in which the *c-fos* promoter controls expression of a *tau-lacZ* reporter construct (FTL mice). DCA (25 μg, s.c.) or vehicle (control) was injected into the nape of the neck of sedated mice. Mice were either allowed to regain consciousness or were kept sedated, and 60 min later the cervical spinal cord was removed for analysis of β-galactosidase in the dorsal horn. In conscious mice receiving vehicle, β-galactosidase was detected in few neurons (Fig. 6C, D). In DCA-treated mice, β-galactosidase was detected in the soma and processes of numerous neurons in laminae I, II, and III of the dorsal horn, as well as in some deeper laminae (Fig. 6C, D). The number of β-

galactosidase-positive neurons in superficial laminae increased from 15 ± 3.8 in vehicle-treated mice to 34 ± 5.3 in DCA-treated mice ($p<0.05$, $n=3$). HC-030031 ($100\text{ mg}\cdot\text{kg}^{-1}$, p.o.), administered 30 min before DCA, prevented DCA-evoked activation of spinal neurons (Fig. 6D). DCA similarly induced β -galactosidase in superficial spinal neurons of anesthetized mice, which indicates that scratching was not necessary for *c-fos* induction (Fig. 6E). Thus, cutaneous DCA activates spinal neurons, and TRPA1 is required for the central transmission of the pruritogenic signal.

BAs cause scratching by TRPA1-dependent mechanisms. To evaluate the contribution of TRPA1 to BA-stimulated scratching, we injected DCA ($25\text{ }\mu\text{g}$, s.c.) into the nape of the neck in wild-type or *trpa1*^{-/-} mice, and quantified scratching for 60 min. In wild-type mice, DCA stimulated a 4-fold increase in scratching over baseline (scratches. 60 min^{-1} : basal, 22.7 ± 5.2 ; DCA, 81.2 ± 8.3 , $p<0.0001$, $n=8-10$ mice) (Fig. 7A). DCA did not cause scratching in *trpa1*^{-/-} mice (21.9 ± 7.6 , $n=10$ mice). To examine the therapeutic potential of a TRPA1 antagonist to treat BA-evoked pruritus, we administered the TRPA1 antagonist HC-030031 ($100\text{ mg}\cdot\text{kg}^{-1}$, p.o.) or vehicle (control) to wild-type mice 30 min before DCA. HC-030031 prevented DCA-evoked scratching (scratches. 60 min^{-1} : vehicle, 103.3 ± 27.2 ; HC-030031, 25.3 ± 14.4 , $p<0.0001$, $n=6$ mice) (Fig. 7B). In contrast, the TRPV1 antagonist AMG-9810 ($40\text{ mg}\cdot\text{kg}^{-1}$, i.p.) did not affect DCA-evoked scratching (scratches. 60 min^{-1} : vehicle, 117.2 ± 10.03 ; AMG-9810, 133.3 ± 17.3 , $p=0.4383$, $n=6$ mice) (Fig. 7C). AMG-9810 prevented cheek wiping responses to capsaicin ($3\text{ }\mu\text{g}$, s.c.), suggesting effective antagonism of TRPV1-mediated nociceptive behavior (wipes. 20 min^{-1} : vehicle, 46.4 ± 7.2 , AMG-9810, 10 ± 3.8 , $p<0.005$, $n=5$ mice) (Supplemental Fig. 4). Thus, DCA causes scratching in mice by a mechanism that requires expression and activation of TRPA1 but not TRPV1.

Endogenous BAs and TRPA1 can induce spontaneous pruritus. Transgenic mice overexpressing mouse TGR5 (*tgr5-tg*) exhibit elevated TGR5 expression in tissues known to express TGR5²⁵ and demonstrate exacerbated spontaneous scratching by unknown mechanisms⁹. Since the circulating levels of BAs fluctuate during feeding and fasting²⁶, we evaluated whether endogenous circulating BAs could be responsible for the exacerbated scratching in *tgr5-tg* mice. We treated *tgr5-tg* mice with the BA sequestrant colestipol ($100\text{ mg}\cdot\text{kg}^{-1}$, b.i.d) or vehicle (control) by gavage for 5 days, and then assessed scratching behavior. Vehicle-treated *tgr5-tg* mice scratched 2.6-fold more frequently than wild-type mice (scratches. 60 min^{-1} : wild-type, 22.7 ± 5.7 ; *tgr5-tg*, 57.1 ± 9.4 , $p<0.005$, $n=7-8$ mice) (Fig. 7D). Colestipol reduced scratching of *tgr5-tg* mice by 2.1-fold (scratches. 60 min^{-1} : *tgr5-tg*, 57.1 ± 9.4 ; colestipol, 27.5 ± 6.6 , $p<0.05$ compared to vehicle-treated *tgr5-tg* mice, $n=7-8$ mice) (Fig. 7D). Colestipol also caused a 2.5-fold reduction in the plasma concentrations of total BAs ($p<0.01$ compared to vehicle, $n=7$ mice) (Fig. 7E). HC-030031 strongly inhibited scratching of *tgr5-tg* mice when compared to vehicle (scratches. 60 min^{-1} : vehicle, 41.3 ± 7.8 ; HC-030031, 9.4 ± 3.0 , $p<0.01$ compared to vehicle-treated *tgr5-tg* mice, $n=8$ mice) (Fig.

7F). Thus, endogenous circulating BAs and TRPA1 are responsible for exacerbated spontaneous scratching in *tgr5-tg*. These results highlight the patho-physiological importance of TGR5- and TRPA1-induced itch caused by endogenous BAs.

Discussion

Our results reveal an essential role for TGR5-induced activation of TRPA1 for the pruritogenic actions of exogenous and endogenous BAs. We report that TGR5 and TRPA1 are co-expressed by a sub-population of cutaneous afferent neurons, and that TGR5 activates TRPA1 *via* G $\beta\gamma$ and PKC (Supplemental Fig. 5). TRPA1 is necessary for BA-evoked release of the pruritogenic neuropeptides in the spinal cord, activation of spinal neurons, and scratching behavior. A major finding is that the exacerbated scratching in mice over-expressing TGR5 is driven by endogenous BAs and requires TRPA1 activation.

TGR5 activates and sensitizes TRPA1. We found that ~7% of cutaneous afferent neurons co-expressed TGR5 and TRPA1, determined by retrograde tracing, immunofluorescence, *in situ* hybridization, and single cell RT-PCR. BAs induced Ca²⁺ signals only in those DRG neurons that responded to the TRPA1 agonist AITC, confirming co-expression of functional TGR5 and TRPA1.

Our results show that BAs, *via* TGR5, activate and sensitize TRPA1. Although TGR5 does stimulate G α_q -dependent mobilization of intracellular Ca²⁺ stores, BAs increased [Ca²⁺]_i in HEK cells and DRG neurons coexpressing TGR5 and TRPA1. This effect was abolished by TRPA1 antagonism or deletion. Thus, BAs stimulate TGR5, which in turn activates TRPA1 to cause an influx of extracellular Ca²⁺ ions. Gallein and GF109203X attenuated BA-evoked activation of TRPA1 in HEK-TGR5+TRPA1 cells and in DRG neurons, which implicates G $\beta\gamma$ and PKC in TGR5-evoked activation of TRPA1. G $\beta\gamma$ also mediates MrgprA3-induced activation of TRPA1 in NG108 cells⁵, either by directly binding to TRPA1²⁰ or through other pathways. PKC can also mediate bradykinin-evoked activation of TRPV1, which in turn activates TRPA1 by a Ca²⁺-dependent process²⁷. However, we did not observe a major role for TRPV1 in BA-evoked Ca²⁺ signaling in DRG neurons. Alternatively, activated TGR5 could generate TRPA1 agonists, which remains to be investigated.

TGR5 can also sensitize TRPA1, since pretreatment of oocytes expressing TGR5 and TRPA1 with DCA amplified AITC-elicited TRPA1 currents. Chelation of intracellular Ca²⁺ ions in oocytes prevented this sensitization, which is consistent with the known ability of Ca²⁺ ions to activate TRPA1²⁸. DCA did not alter TRPA1 currents in oocytes expressing TRPA1 alone or increase [Ca²⁺]_i in HEK-TRPA1 cells. Thus, BAs cannot directly regulate TRPA1.

TRPA1 is required for TGR5-dependent itch. We report that TRPA1 is necessary for the central transmission of the pruritogenic signals from cutaneous BAs. TLCA stimulated GRP and NPPB release in the spinal cord, consistent with involvement of GRP in TGR5-dependent scratching⁹. HC-030031

prevented TLCA-stimulated GRP and NPPB release, which reveals a key role for TRPA1 in BA-induced release of neuropeptides that mediate itch transmission in the dorsal horn. TRPA1 deletion and antagonism also prevented cutaneous DCA-evoked activation of spinal neurons, revealed by *c-fos* expression, and scratching. Although TGR5 was co-expressed in primary sensory neurons with both TRPA1 and TRPV1, TRPV1 antagonism or deletion had no effect on DCA-evoked scratching. This result is consistent with the retention of DCA-evoked Ca^{2+} signaling in neurons from *trpv1*^{-/-} mice. With regard to its dependency for activation of TRPA1, but not TRPV1, for neuronal activation and scratching, TGR5 resembles MrgprA3 and MrgprC11, which also activate TRPA1 to induce itch⁵.

A key finding is that the BA sequestrant colestipol inhibits exacerbated spontaneous scratching in gain-of-function *tgr5-tg* mice. BAs that are secreted into the intestinal lumen during feeding are absorbed in the ileum and colon, and the circulating levels of BAs wax and wane during feeding and fasting²⁶. Our observation that treatment of *tgr5-tg* mice with a BA sequestrant reduced both spontaneous scratching and circulating BA levels by ~ 50% suggests that endogenous BAs are sufficient to drive exacerbated scratching in mice that overexpress TGR5. HC-030031 reduced spontaneous scratching of *tgr5-tg* mice to that observed under basal conditions in wild-type mice, which reveals a requirement for TRPA1 for the pruritogenic actions of endogenous BAs.

Contributions of BAs, TGR5 and TRPA1 to cholestatic pruritus. The contribution of BAs to cholestatic pruritus is debatable. There are increased circulating and tissue levels of BAs in cholestatic patients^{11,12}, injection of BAs into the skin causes scratching in humans¹⁴, and BA sequestrants are a treatment for cholestatic pruritus¹³. However, scratching severity does not correlate with circulating BAs levels in patients with cholestatic disease, and other factors have been implicated in cholestatic itch, including lysophosphatidic acid and opioids^{29,30}. Our finding that *tgr5-tg* mice exhibit spontaneous pruritus that depends on endogenous BAs suggests that the pathological upregulation of TGR5 alone, in the absence of elevated levels of BAs, may be sufficient to induce pruritus. Whether TGR5 is upregulated in patients with pruritus remains to be examined. We found that TRPA1 antagonism prevents exacerbated scratching of *tgr5-tg* mice. Thus, TRPA1 antagonists, in addition to TGR5 antagonists, may be considered to be new treatments for pruritus that accompanies liver diseases and other conditions such as pregnancy, where certain upregulated progesterone metabolites may also activate TGR5³¹. These possibilities deserve further attention. Given intractable nature of the severe pruritus that accompanies hepatic diseases, potentially leading to liver transplantation, the TGR5/TRPA1 pathway may be a therapeutic target for the histamine-independent chronic itch in which BAs are involved.

Figure Legends

Figure 1. Localization and expression of TGR5-IR, NeuN-IR and TRPA1 mRNA in cutaneous afferent neurons. **A.** Co-localization of NeuN-IR and TGR5-IR in DiI-positive cutaneous afferent DRG neurons (arrows). Scale, 100 μm . **B.** Proportion of DiI-positive neurons with (TGR5+ve) or without (TGR5-ve) co-expression of TGR5-IR (889 or 1653 neurons, 6 mice). **C.** Co-localization of Hu-C/D-IR, TGR5-IR and TRPA1 mRNA in DiI-positive cutaneous afferent DRG neurons (arrows). Merged images show TGR5-IR + TRPA1 mRNA (left) and DiI + TGR5-IR + TRPA1 mRNA (right). Scale, 100 μm . **D.** Proportion of all neurons or of DiI-positive neurons expressing TGR5-IR alone or TGR5-IR + TRPA1 mRNA (1850 neurons, 6 mice). **E.** Single cell RT-PCR of small diameter, DiI-positive, cutaneous afferent neurons. Transcripts of TGR5, TRPA1, TRPV1, and β -actin were amplified. Results from 17 neurons are shown (60 neurons, 6 mice). Red box denotes co-expression of TGR5, TRPA1 and TRPV1. RT, reverse transcriptase. **F.** Venn diagram indicating the proportion of small diameter, Di-positive cutaneous afferent neurons expressing TRG5, TRPA1 and TRPV1.

Figure 2. BA and TGR5-induced activation and sensitization of TRPA1 in HEK293 cells. **A-D.** $[\text{Ca}^{2+}]_i$ measured in HEK-TGR5 and HEK-TGR5+TRPA1 cells treated with vehicle (Veh) or DCA (100 μM) and then AITC (100 μM). Some cells were treated with gallein (**B**), GF-109203X (GFX, **C**), H-89 or HC-030031 (**D**). **E, F.** Pooled results showing maximal increase in $[\text{Ca}^{2+}]_i$ over basal. Triplicate measurements, 3-8 independent experiments, $*P < 0.05$ compared to vehicle (**E**) or AITC (**F**) in HEK-TGR5+TRPA1 cells.

Figure 3. BA and TGR5-induced activation of TRPA1 currents in *Xenopus laevis* oocytes. Oocytes expressing TRPA1 alone or TRPA1 and TGR5 were stimulated with the TRPA1 agonist AITC (50 μM , black bar) and the TRPA1 antagonist HC-030031 (open bar). TGR5 was activated by DCA (500 μM , gray bar). **A, B.** Representative whole-cell current traces of oocytes expressing TRPA1 (**A**) or TRPA1 and TGR5 (**B**). Oocytes were treated with vehicle or DCA 30 s before AITC. **C, D.** Change in AITC currents ($\Delta I_{\text{AITC peak}}$) in oocytes treated with DCA (+) or vehicle (-) (**C**). $\Delta I_{\text{AITC peak}}$ in oocytes preincubated for 3 h in BAPTA-AM or vehicle and subsequently treated with DCA (+) or vehicle (-) (**D**). Numbers inside the columns indicate the number of individual oocytes measured. N indicates the number of batches of oocytes. $***P < 0.001$.

Figure 4. TGR5- and TRPA1-dependent BA signaling in DRG neurons. $[\text{Ca}^{2+}]_i$ was measured in small diameter neurons from WT mice (**A**), WT mice in Ca^{2+} -free medium (**B**), *tgr5*^{-/-} mice (**C**), *trpa1*^{-/-} mice (**D**), and WT mice treated with the TRPA1 antagonist HC-030031 (**E**). They were challenged sequentially with AITC (100 μM), DCA (100 μM) and capsaicin (CAP, 1 μM). Responses of KCl (50 mM) - responsive neurons are shown. **F.** Pooled data showing the proportion of DCA- or TLCA-responsive neurons in the different experimental groups. In A-E, each line represents a single neuron. F represents pooled data from 2281 neurons, n=17 mice. $**P < 0.01$ to DCA in WT.

Figure 5. The proportion of DRG neurons responding to BAs and agonists of TRP channels. $[Ca^{2+}]_i$ was measured in small diameter neurons from wild-type (WT) mice (**A, F**), wild-type mice in Ca^{2+} -free medium (**B**), *tgr5^{-/-}* mice (**C**), *trpa1^{-/-}* mice (**D**), WT mice treated with the TRPA1 antagonist HC-030031 (**E**). They were challenged sequentially with AITC (100 μ M), DCA (A-E) or TLCA (F) (both 100 μ M), capsaicin (CAP, 1 μ M), and finally KCl (50 mM). The proportion of small diameter neurons that responded to the combinations of AITC, DCA or TLCA, and capsaicin are shown. Pooled data from 184-1435 neurons, n=5-12 mice.

Figure 6. Contributions of TRPA1 to BA-evoked release of pruritogenic neuropeptides and activation of spinal neurons. **A, B.** Release of GRP-IR (**A**) and NPPB-IR (**B**) from superfused slices of rat spinal cord under basal conditions and after stimulation with TLCA (500 μ M, 60 min). Tissues were preincubated with vehicle or HC-030031 (50 μ M). n=4, * P <0.05. **C-E.** Expression of *c-fos* in neurons in the dorsal horn of *c-fos* reporter mice. **C.** Photomicrographs of the dorsal horn of the spinal cord (C1-C7) 60 min after injection of DCA (25 μ g, s.c.) or vehicle to the nape of the neck of conscious mice. Scale: left panel 100 μ m, right panel 25 μ m **D.** Quantification of *c-fos*-expressing neurons in superficial laminae of the spinal cord (C1-C7) 60 min after injection of DCA or vehicle. **E.** Quantification of *c-fos*-expressing neurons 60 min after injection of DCA or vehicle in anesthetized mice. Sub-groups of the DCA-treated mice were pretreated with HC-030031 or vehicle 30 min before DCA. n=3 mice, * P <0.05 to vehicle.

Figure 7. Contributions of TRPA1 to scratching evoked by exogenous and endogenous BAs. **A-C.** DCA-evoked scratching in wild-type (WT) and *trpa1^{-/-}* mice. DCA was injected to the nape of the neck (25 μ g s.c.) and scratching was measured for 60 min in wild-type mice and *trpa1^{-/-}* mice (**A**), in wild-type mice pretreated with HC-030031 or vehicle (**B**), and in wild-type mice pretreated with AMG-9810 or vehicle and in *trpv1^{-/-}* mice (**C**). **D-F.** Scratching and serum BAs levels in *tgr5-tg* mice. *tgr5-tg* mice were treated with colestipol or vehicle for 5 days before measurement of scratching (**D**) and plasma concentrations of total BAs (**E**). Scratching was also measured in *tgr5-tg* mice pretreated with HC-030031 or vehicle (**F**). n=6-10 mice, * P <0.05, ** P <0.01 to untreated wild-type mice (A-C) or vehicle (D-F).

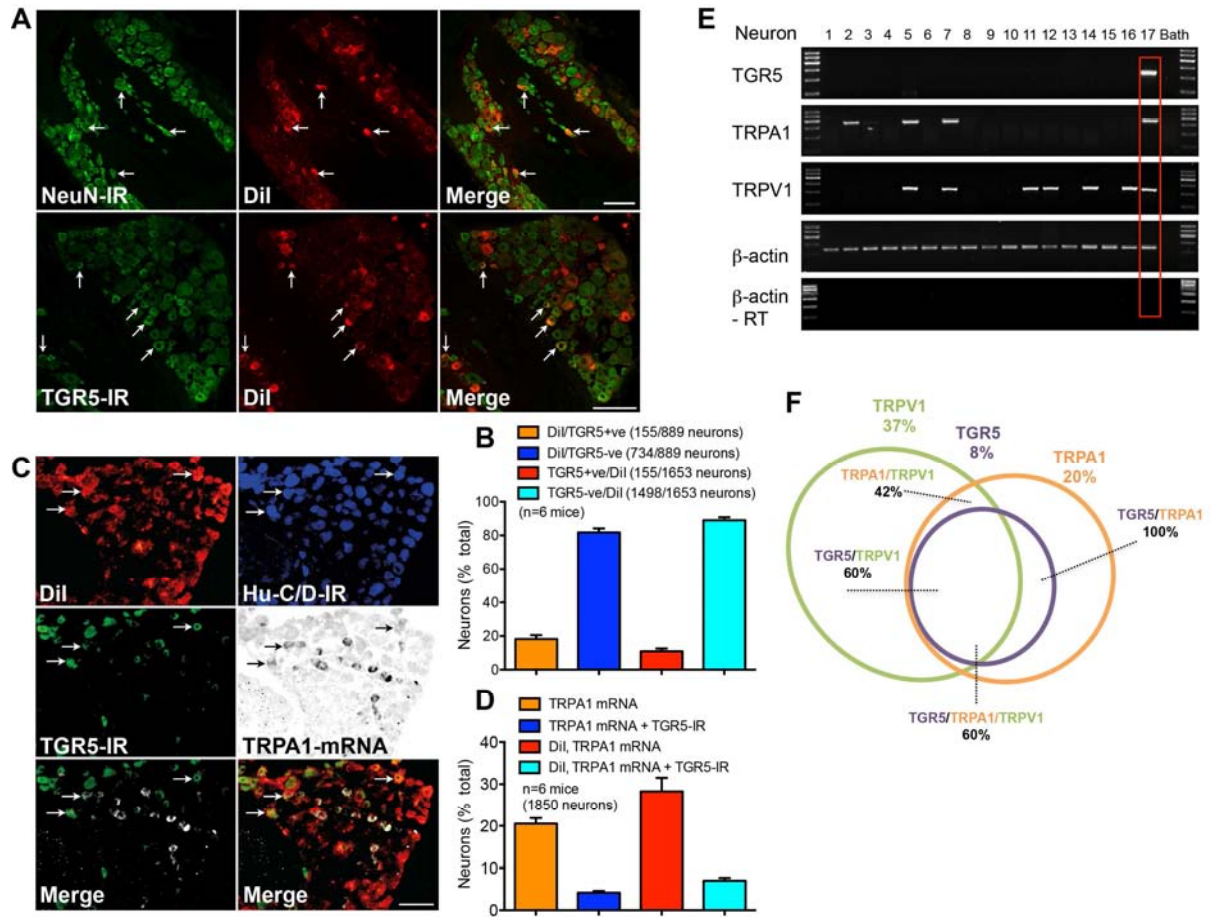
References

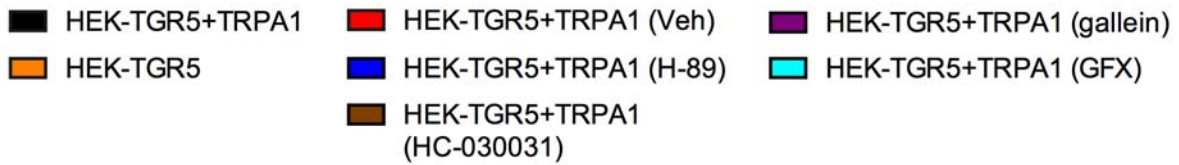
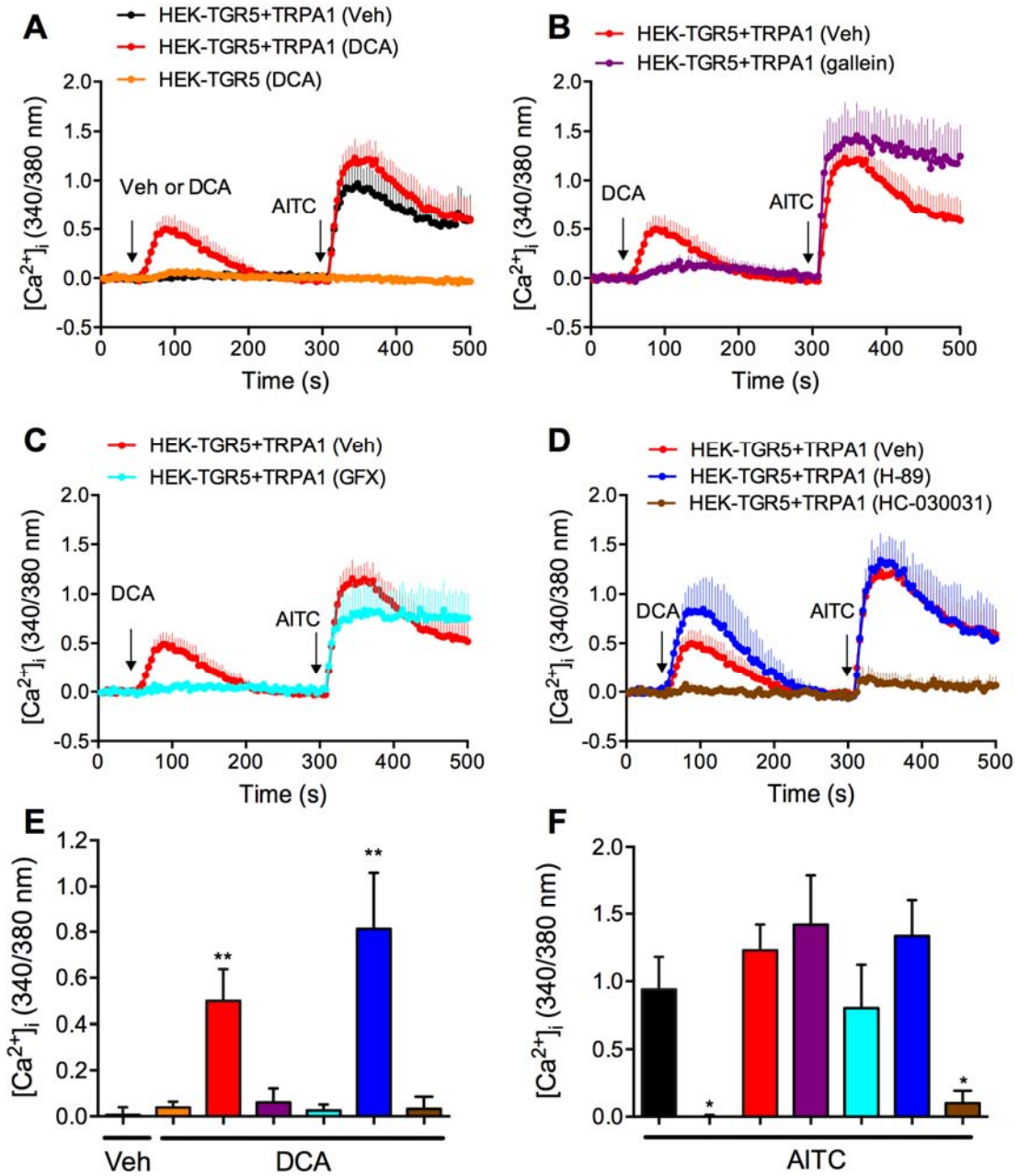
1. Ikoma A, Steinhoff M, Stander S, et al. The neurobiology of itch. *Nat Rev Neurosci* 2006;7:535-547.
2. Imamachi N, Park GH, Lee H, et al. TRPV1-expressing primary afferents generate behavioral responses to pruritogens via multiple mechanisms. *Proc Natl Acad Sci USA* 2009;106:11330-11335.
3. Liu Q, Tang Z, Surdenikova L, et al. Sensory neuron-specific GPCR Mrgprs are itch receptors mediating chloroquine-induced pruritus. *Cell* 2009;139:1353-1365.
4. Steinhoff M, Neisius U, Ikoma A, et al. Proteinase-activated receptor-2 mediates itch: a novel pathway for pruritus in human skin. *J Neurosci* 2003;23:6176-6180.

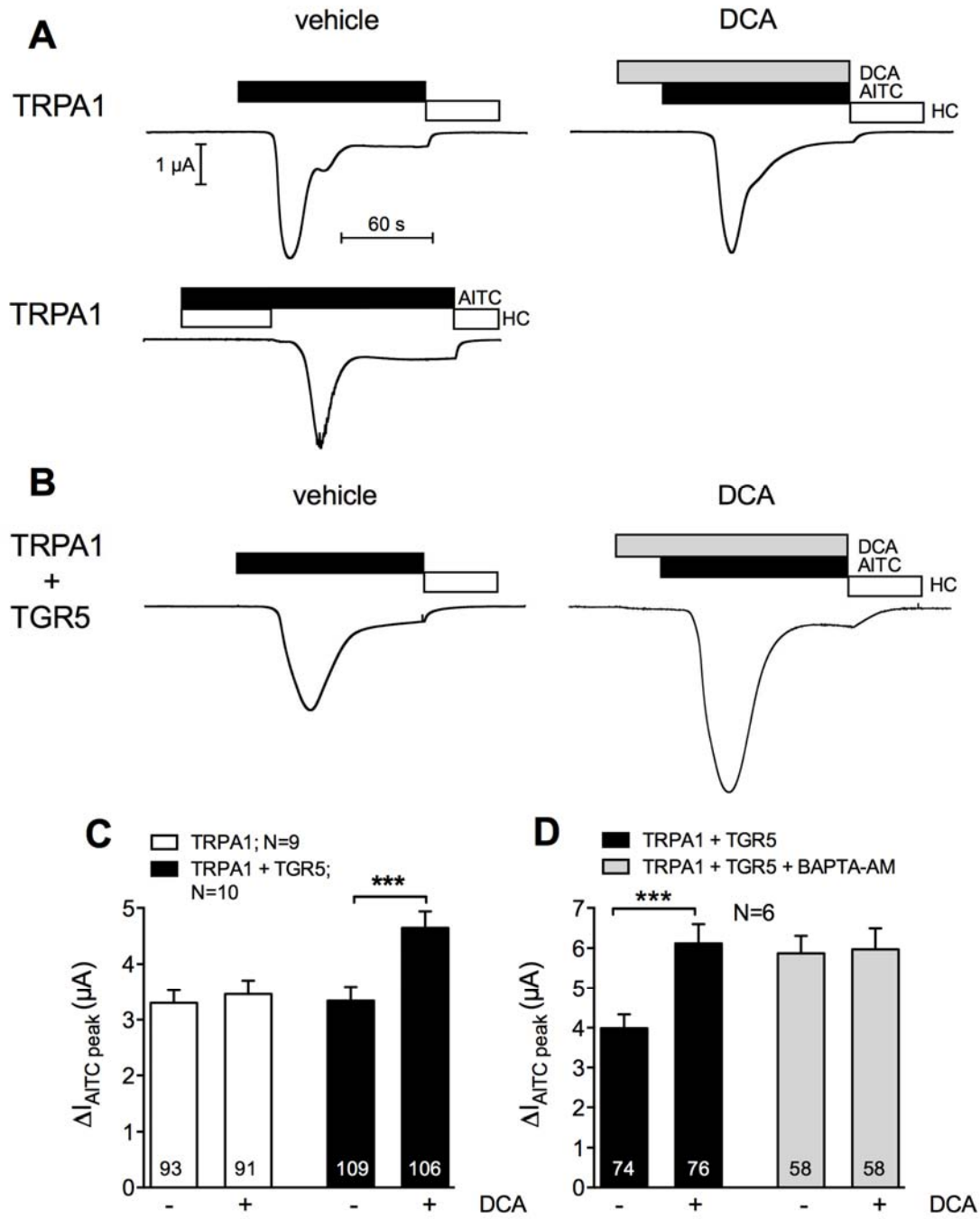
5. Wilson SR, Gerhold KA, Bifolck-Fisher A, et al. TRPA1 is required for histamine-independent, Mas-related G protein-coupled receptor-mediated itch. *Nat Neurosci* 2011;14:595-602.
6. Wilson SR, Nelson AM, Batia L, et al. The ion channel TRPA1 is required for chronic itch. *J Neurosci* 2013;33:9283-9294.
7. Sun YG, Chen ZF. A gastrin-releasing peptide receptor mediates the itch sensation in the spinal cord. *Nature* 2007;448:700-703.
8. Mishra SK, Hoon MA. The cells and circuitry for itch responses in mice. *Science* 2013;340:968-971.
9. **Alemi F, Kwon E**, Poole DP, et al. The TGR5 receptor mediates bile acid-induced itch and analgesia. *J Clin Invest* 2013;123:1513-1530.
10. EASL Clinical Practice Guidelines: management of cholestatic liver diseases. *J Hepatol* 2009;51:237-267.
11. Magyar I, Loi HG, Feher T. Plasma bile acid levels and liver disease. *Acta Med Acad Sci Hung* 1981;38:109-115.
12. Schoenfield LJ, Sjorvall J, Perman E. Bile acids on the skin of patients with pruritic hepatobiliary disease. *Nature* 1967;213:93-94.
13. Mela M, Mancuso A, Burroughs AK. Review article: pruritus in cholestatic and other liver diseases. *Aliment Pharmacol Ther* 2003;17:857-870.
14. Kirby J, Heaton KW, Burton JL. Pruritic effect of bile salts. *Br Med J* 1974;4:693-695.
15. Cho HJ, Callaghan B, Bron R, et al. Identification of enteroendocrine cells that express TRPA1 channels in the mouse intestine. *Cell Tiss Res* 2014.
16. Poole DP, Godfrey C, Cattaruzza F, et al. Expression and function of the bile acid receptor GpBAR1 (TGR5) in the murine enteric nervous system. *Neurogastroenterol Motil* 2010;22:814-825, e227-818.
17. Haerteis S, Krappitz M, Diakov A, et al. Plasmin and chymotrypsin have distinct preferences for channel activating cleavage sites in the gamma subunit of the human epithelial sodium channel. *J Gen Phys* 2012;140:375-389.
18. Wilson Y, Nag N, Davern P, et al. Visualization of functionally activated circuitry in the brain. *Proc Natl Acad Sci USA* 2002;99:3252-3257.
19. Shimada SG, LaMotte RH. Behavioral differentiation between itch and pain in mouse. *Pain* 2008;139:681-687.
20. Dascal N. Ion-channel regulation by G proteins. *Trends in endocrinology and metabolism: TEM* 2001;12:391-398.
21. Amadesi S, Cottrell GS, Divino L, et al. Protease-activated receptor 2 sensitizes TRPV1 by protein kinase C epsilon- and A-dependent mechanisms in rats and mice. *J Phys* 2006;575:555-571.
22. Jensen DD, Godfrey CB, Niklas C, et al. The bile acid receptor TGR5 does not interact with beta-arrestins or traffic to endosomes but transmits sustained signals from plasma membrane rafts. *J Biol Chem* 2013;288:22942-22960.
23. Kawamata Y, Fujii R, Hosoya M, et al. A G protein-coupled receptor responsive to bile acids. *J Biol Chem* 2003;278:9435-9440.
24. Maruyama T, Miyamoto Y, Nakamura T, et al. Identification of membrane-type receptor for bile acids (M-BAR). *Biochem Biophys Res Commun* 2002;298:714-719.
25. Thomas C, Gioiello A, Noriega L, et al. TGR5-mediated bile acid sensing controls glucose homeostasis. *Cell Metab* 2009;10:167-177.
26. Angelin B, Bjorkhem I. Postprandial serum bile acids in healthy man. Evidence for differences in absorptive pattern between individual bile acids. *Gut* 1977;18:606-609.
27. Bautista DM, Jordt SE, Nikai T, et al. TRPA1 mediates the inflammatory actions of environmental irritants and proalgesic agents. *Cell* 2006;124:1269-1282.
28. Jordt SE, Bautista DM, Chuang HH, et al. Mustard oils and cannabinoids excite sensory nerve fibres through the TRP channel ANKTM1. *Nature* 2004;427:260-265.

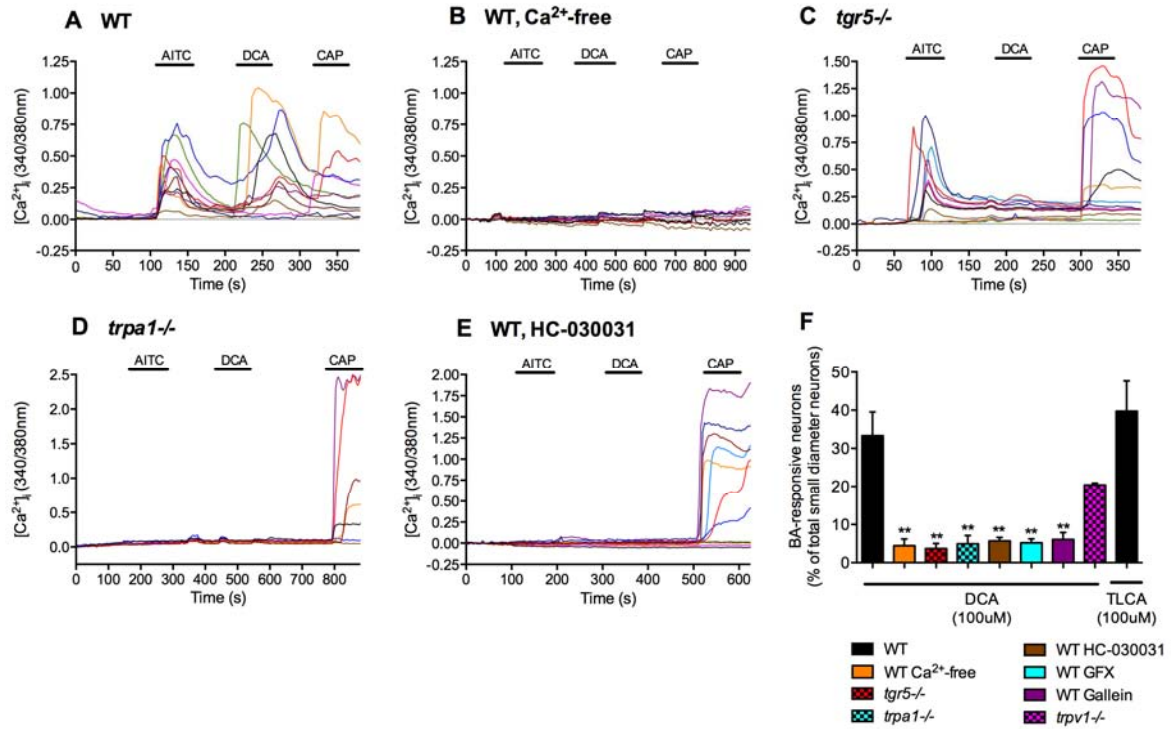
29. Bergasa NV. The itch of liver disease. *Seminars in cutaneous medicine and surgery* 2011;30:93-98.
30. Kremer AE, Martens JJ, Kulik W, et al. Lysophosphatidic acid is a potential mediator of cholestatic pruritus. *Gastroenterology* 2010;139:1008-1018, 1018 e1001.
31. Papacleovoulou G, Abu-Hayyeh S, Nikolopoulou E, et al. Maternal cholestasis during pregnancy programs metabolic disease in offspring. *J Clin Invest* 2013;123:3172-3181.

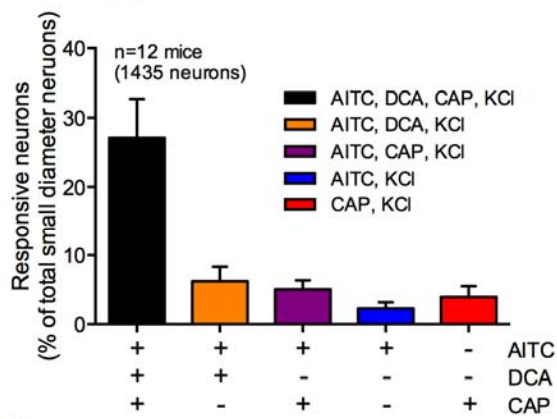
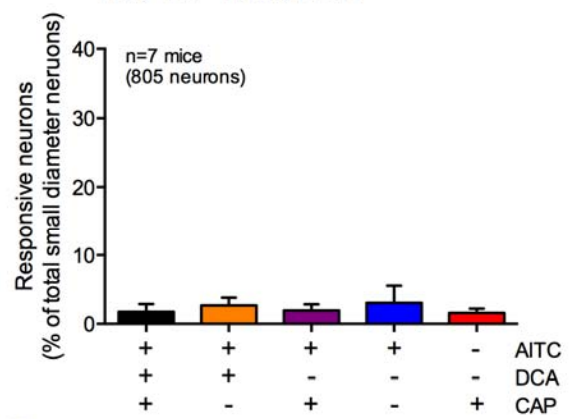
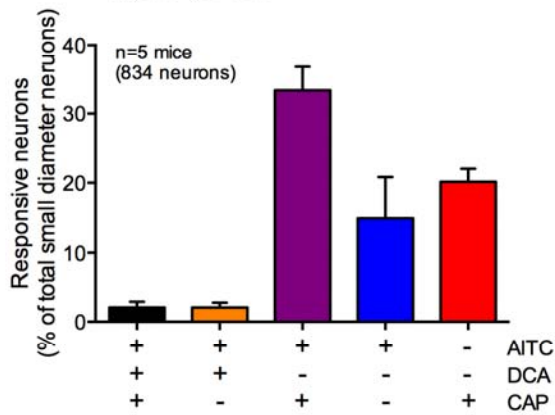
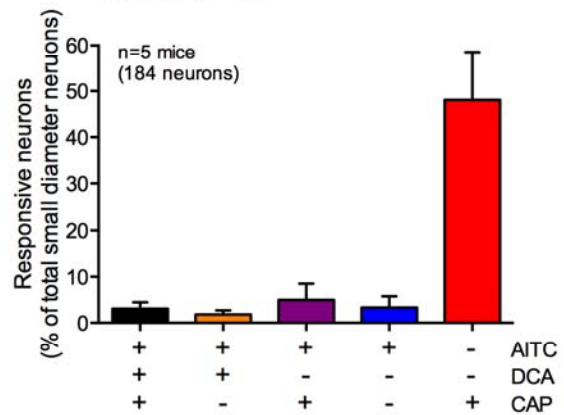
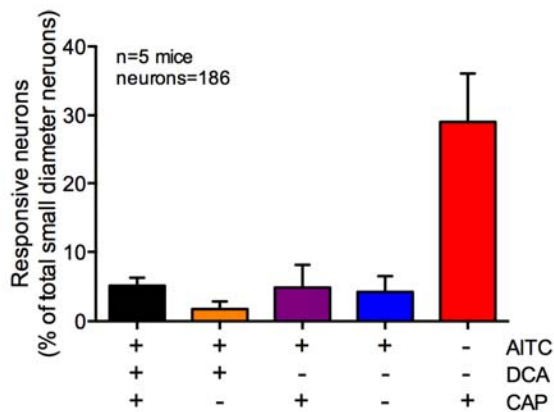
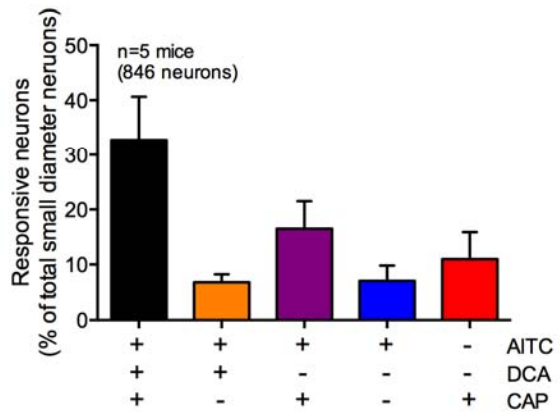
Author names in bold designate shared co-first authors

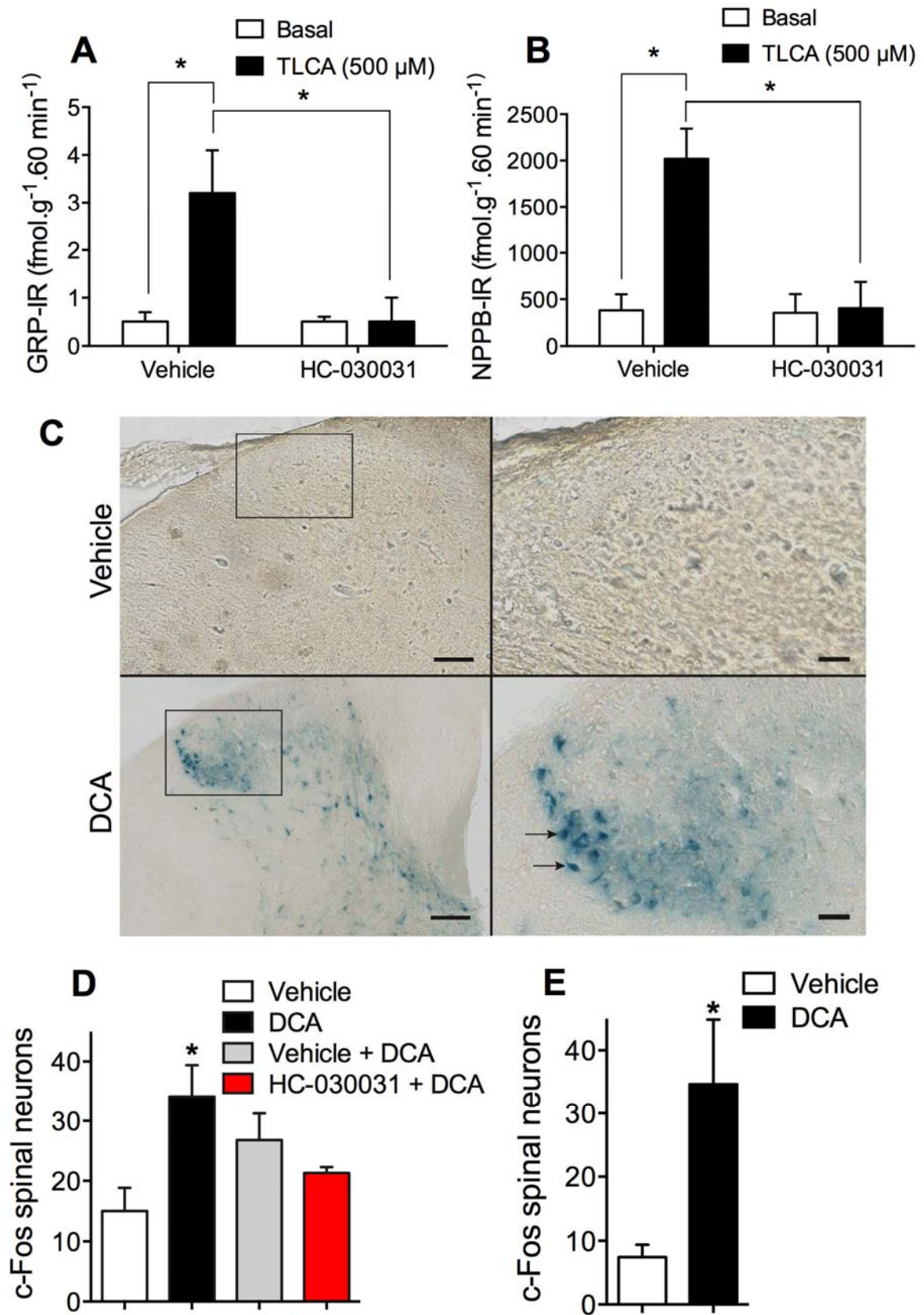


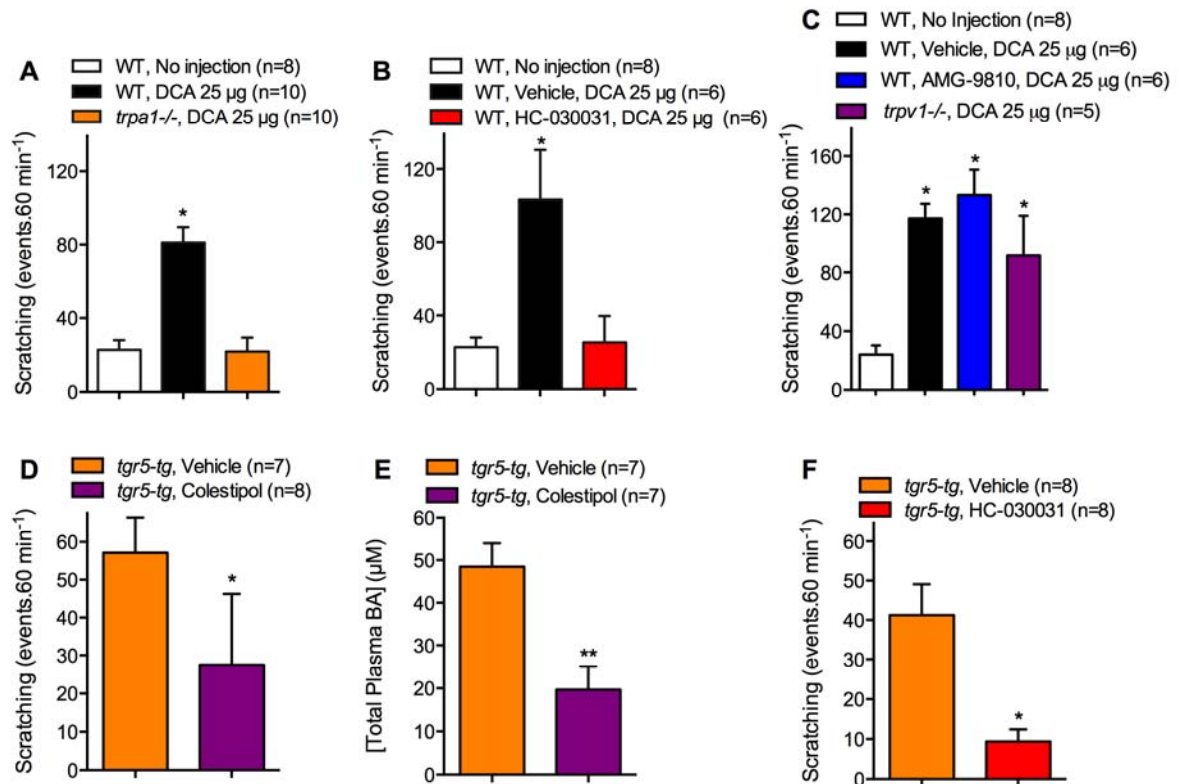






A WT, DCA**B WT, Ca²⁺-free, DCA****C *tgr5*^{-/-}, DCA****D *trpa1*^{-/-}, DCA****E WT, HC-030031, DCA****F WT, TLCA**





Supplemental Materials and Methods

Animals. Animal Ethics Committees of Monash University, the University of Erlangen-Nürnberg and the University of Florence approved all studies on animals. C57BL/6 mice were from Monash Animal Research Platform. *Tgr5^{-/-}*, *tgr5-tg*, *trpa1^{-/-}*, *trpv1^{-/-}* and *fos-tau-lacZ* mice have been described¹⁻⁴. Male mice (6-10 weeks) were used. Male Sprague-Dawley rats (180-200 g) were from Harlan Laboratories (Italy). Mice and rats were maintained in a temperature-controlled environment with a 12 h light/dark cycle and free access to food and water. Mice and rats were killed by anesthetic overdose and bilateral thoracotomy.

Materials. HC-030031, gallein, and GF109203X were from Tocris Biosciences (Minneapolis, MN, USA) and AMG-9810 was from Amgen Inc (Thousand Oaks, CA, USA). Unless stated otherwise, other reagents were from Sigma-Aldrich (St Louis, MO, USA). The concentrations of inhibitors and antagonists were selected from published studies examining regulation of TRP channel activation⁵⁻⁷.

Retrograde tracing. Mice (C57BL/6) were anesthetized with 5% isoflurane. A single intradermal injection of 1,1'-Diocadecyl-3,3',3'-Tetramethylindocarbocyanine Perchlorate (DiI, 2%, 10 μ l) was made to the nape of the neck. Mice recovered for 7 days before tissue collection.

Immunofluorescence. After retrograde tracing, DRG (C1-C7) were removed and fixed in 4% paraformaldehyde (PFA), 100 mM PBS, pH 7.4 (overnight, 4°C). DRG were washed in PBS and cryoprotected in 30% sucrose, PBS, 0.1% sodium azide (overnight, 4°C). DRG were embedded in TissueTek Optimal Cutting Temperature compound (OCT, Sakura Finetek, Torrance, CA), and 12 μ m frozen sections were prepared, with every third section mounted onto slides. Sections were incubated in blocking buffer (10% normal horse serum, 0.1% Triton X-100 in PBS containing 0.1% sodium azide; 1 h, room temperature), and were incubated with rabbit anti-TGR5 (1:500,⁸) or rabbit anti-NeuN (FOX3) (1:2,000, Abcam, Cambridge, UK, #104225) in blocking buffer (overnight, 4°C). Sections were washed in PBS and incubated with Alexa 488-conjugated donkey anti-rabbit IgG (1:1,000, Jackson ImmunoResearch, Westgrove, PA, USA) (1 h, room temperature). Sections were mounted in Prolong Gold (Invitrogen, Carlsbad, CA). Sections were observed using a Leica TCS SP8 confocal microscope. Images (1024x1024 pixels) were collected as z-stacks of the full diameter and thickness of each section. Ten sections were imaged per mouse, and images lacking detectable DiI were excluded. Z-stacks for individual channels were maximally projected using ImageJ (NIH). The threshold of images was set and DiI- or TGR5-positive neurons were identified independently and defined as regions of interest (ROIs). The ROIs were then combined and the relative overlap between DiI- and TGR5-positive neuronal populations was determined and expressed as a percentage of the total populations.

In-situ hybridization and immunohistochemistry. A plasmid to prepare antisense cRNA complimentary to mouse TRPA1 mRNA was constructed using a partial mouse TRPA1 cDNA of 918 bp that was

amplified by RT-PCR from mouse DRG RNA using forward primer 5'acttctctggattacaacaatgctctg3' and reverse primer 3'attccacttgctgtgcatctgttc5' ⁹. The PCR product was cloned into the pCRII-TOPO vector (Invitrogen) and its orientation was confirmed using M13 forward and reverse primers. Linear templates were prepared by PCR using M13 forward and reverse primers. Antisense and control sense digoxigenin-labeled cRNA was prepared by *in vitro* transcription with T7 and SP6 RNA polymerases (Roche Diagnostics, Indianapolis, IN), respectively. After retrograde tracing, cervical DRG were removed and fixed in 4% PFA (overnight, 4°C). The ganglia were washed in diethylpyrocarbonate (DEPC) PBS, 4°C, incubated in 30% sucrose in DEPC-PBS (4 h, 4°C), embedded in OCT, and 12 µm frozen sections were prepared. Since the DiI fluorescence did not persist after the *in situ* hybridisation protocol, it was imaged beforehand. Sections were hybridised with TRPA1 probe in hybridisation buffer (50% formamide, 4x standard salt concentration [SSC]), pH 7.5, 10% dextran sulphate, 1x Denhardt's solution, 0.1 mg.ml⁻¹ yeast RNA) (overnight, 60°C) ¹⁰. Bound probe was detected with alkaline phosphatase (AP)-conjugated sheep-anti-digoxigenin (DIG) Fab' using the NBD/BCIP substrate (Roche Diagnostics). Sections were then incubated with rabbit anti-TGR5 (1:500) or mouse anti-HuC/D (1:1,000, Invitrogen) (overnight, 4°C). Sections were washed and incubated with Alexa 488- or Alexa 647-conjugated donkey anti-rabbit IgG (Invitrogen) (1:1,000, 2 h, room temperature). Sections were observed using a Zeiss Axioskope.Z1 fluorescence microscope. The intensities of *in situ* hybridization and fluorescence signals and the extent of overlap were quantified using the ImageProPlus software (Media Cybernetics, Silver Spring, MD, USA), as described ¹¹.

Single cell RT-PCR. After retrograde tracing, DRG were collected from all spinal levels, and were dissociated as described ¹². Dissociated neurons were plated onto poly D-lysine- (0.1 mg.ml⁻¹) and laminin- (0.004 mg.ml⁻¹) coated cover slips, and were incubated in Leibovitz's L-15 medium containing 10% FBS in a humidified incubator (8 h, 37°C). Individual DiI-positive small diameter (<25 µm) neurons were selected and drawn into a glass-pipette (tip diameter 25-100 µm) by applying negative pressure ¹³. The pipette tip was broken in a PCR tube containing 1 µl of resuspension buffer and RNase inhibitor (RNaseOUT, 2 U.µl⁻¹, Invitrogen) and snap frozen. PCR reactions used the following intron-spanning mouse primers: TGR5 outer primer forward 5'-cactgcctctctctctgtcc-3', reverse 5'-tcaagtccagggtcaaatctctg-3'; TGR5 inner primer forward 5'-tgctctctctgtgtgtgg-3', reverse 5'-gtccctcttggtctctctc-3'; TRPV1 forward 5'-tcaccgtcagctctgtgtgc-3', reverse 5'-gggtcttgaactcgtctgc-3'; TRPA1 forward 5'-ggagcagacatcaacagcac-3', reverse 5'-gcaggggagcattcttatc-3'; or b-actin forward 5'-ctggctcgcacaacggctcc-3', 5'-reverse gccagatcttccatg-3' ¹². As a negative control, superfusing fluid from the vicinity of the collected cells was amplified, or RT was omitted. Products were separated by electrophoresis (2% agarose), stained using ethidium bromide, and sequenced to confirm identity.

Cell lines. HEK293 cell lines stably expressing human TGR5 have been described⁸. HEK293 cells expressing human TRPA1 were generated using a tetracycline-inducible system. Briefly, Flp-In™ T-Rex™ HEK293 cells were transfected with pcDNA5/FRT/TO containing TRPA1 using Lipofectamine 2000 (Invitrogen). Cells were grown in Dulbecco's Modified Eagle's Medium (DMEM) containing 10% tetracycline-free fetal bovine serum (FBS), blasticidin (5 $\mu\text{g}\cdot\text{ml}^{-1}$) and hygromycin (100 $\mu\text{g}\cdot\text{ml}^{-1}$). To generate cells co-expressing TRPA1 and TGR5, human TGR5 was cloned into pcDNA3.1 neo and then co-transfected into the HEK-TRPA1 cells using a calcium phosphate-DNA co-precipitation method. In brief, cells were incubated in 125 mM CaCl_2 plus HBSS with 1 μg TGR5 pcDNA3.1 overnight at 37°C and 5% CO_2 . The transfection medium was replaced with selection medium (10% FBS, 5 $\mu\text{g}\cdot\text{ml}^{-1}$ blasticidin, 100 $\mu\text{g}\cdot\text{ml}^{-1}$ hygromycin, 400 $\mu\text{g}\cdot\text{ml}^{-1}$ G418) and single clones isolated by limiting dilution. The clones were grown under selection, assayed for cAMP responses to the TGR5 agonist DCA, and one clone was selected based on its robust response. Cells were maintained in DMEM containing 10% tetracycline-free fetal FBS, 1% penicillin and streptomycin, 100 $\mu\text{g}\cdot\text{ml}^{-1}$ hygromycin, 400 $\mu\text{g}\cdot\text{ml}^{-1}$ G418 and 5 $\mu\text{g}\cdot\text{ml}^{-1}$ blasticidin. To induce the expression of TRPA1, HEK-TRPA1 and HEK-TRPA1-TGR5 cells were incubated with tetracycline (100 $\text{ng}\cdot\text{ml}^{-1}$) for 16 h before experiments.

$[\text{Ca}^{2+}]_i$ assays in HEK cells. HEK-TGR5, HEK-TRPA1 and HEK-TRPA1-TGR5 cell lines were plated onto poly-D-lysine-coated 96 well plates (30,000 cells per well). Cells were loaded with Fura-2/AM (1.6 μM) in assay buffer (mM: NaCl 150, KCl 2.6, CaCl_2 0.1, MgCl_2 1.18, D-glucose 10, HEPES 10, pH 7.4) containing 4 mM probenecid and 0.5% BSA for 1 h at 37°C. Fluorescence were measured at 340 nm and 380 nm excitation with 530 nm emission using a FlexStation Microplate Reader (Molecular Devices, Sunnyvale, CA). Results are expressed as the 340/380 nm ratio, which is proportional to $[\text{Ca}^{2+}]_i$. To investigate the potential functional coupling between TGR5 and TRPA1, cells were challenged with DCA (100 μM , 5 min) and then AITC (100 μM , 5 min). To investigate the mechanism of TGR5 and TRPA1 functional coupling, cells were incubated with H89 (10 μM , PKA inhibitor), GF109203X (10 μM , PKC inhibitor), gallein (100 μM , $\text{G}\beta\gamma$ inhibitor), or vehicle (control) (60 min preincubation and inclusion through assays).

Isolation and culture of DRG neurons. DRG were removed from all spinal levels from C57BL/6J, *tgr5*^{-/-} and *trpa1*^{-/-} mice, and were dissociated as described¹². Neurons were plated onto poly D-lysine- (0.1 $\text{mg}\cdot\text{ml}^{-1}$) and laminin- (0.004 $\text{mg}\cdot\text{ml}^{-1}$) coated glass coverslips for Ca^{2+} assays or onto poly-D-lysine- and laminin-coated 96 well plates for ERK1/2 and cAMP assays. Neurons were cultured for 24 h before assays.

$[\text{Ca}^{2+}]_i$ assays in DRG neurons. Neurons were loaded with Fura-2-AM (2 μM) in assay buffer (mM: NaCl 150, KCl 2.6, CaCl_2 0.1, MgCl_2 1.18, D-glucose 10, HEPES 10, pH 7.4) containing 4 mM probenecid and 0.5% BSA for 30 min at 37°C. Neurons were mounted in an open chamber and were observed using a Leica DMI6000B microscope with a HC PL APO 20x NA0.75 objective. Fluorescence was measured at

340 nm and 380 nm excitation and 530 nm emission using an Andor iXon 887 camera (Andor, Ireland) and MetaFluor v7.8.0 software (Molecular Devices). Neurons were challenged sequentially with AITC (100 μ M), DCA (100 μ M), capsaicin (1 μ M), and KCl (50 mM). In some experiments, neurons were incubated with GF109203X (10 μ M), gallein (100 μ M), HC-030031 (100 μ M) or vehicle (control) (30 or 60 min preincubation and inclusion throughout), or were assayed in Ca^{2+} -free buffer containing 2 mM EDTA. Images were analyzed using a custom journal in MetaMorph v7.8.2 software (Molecular Devices). A maximum intensity image was generated and projected through time to generate an image of all cells. Cells were segmented and binarized from this image using the Multi Wavelength Cell Scoring module on the basis of size and fluorescence intensity. Neurons of interest ($< 25 \mu\text{m}$ diameter) were selected, and responsive neurons were defined as those with an increase in fluorescence intensity standard deviation of >1.5 fold over the global baseline intensity standard deviation for all time points.

ERK1/2 activation in DRG neurons. Neurons were serum-starved for 6 h before assay. Neurons were challenged with DCA (100 μ M) or phorbol 12,13-dibutyrate (PDBu, 200 nM, positive control) for 30 min at 37°C, and lysed in 30 μ l 0.3% Tween 20, 5 mM HEPES, 0.1% BSA in water, pH 7.4. Activation of ERK1/2 was assessed using the AlphaScreen SureFire phospho-ERK assay (PerkinElmer Life Sciences).

cAMP accumulation in DRG neurons. Neurons were serum-starved for 6 h before assay. Medium was replaced with activation buffer (phenol red-free DMEM containing 5 mM HEPES, 0.1% BSA, 1 mM 3-isobutyl-1-methylxanthine) for 45 min. Neurons were challenged with DCA (100 μ M) or forskolin (10 μ M, positive control) for 30 min at 37°C, and lysed. Accumulation of cAMP was assessed using the AlphaScreen cAMP assay (PerkinElmer Life Sciences).

Measurement of TRPA1 currents in Xenopus laevis oocytes. Oocytes were collected from *Xenopus laevis* as described¹⁴. Defolliculated stage V-VI oocytes were injected (Nanoject II automatic injector, Drummond) with cRNA encoding human TRPA1 alone (0.5 ng) or both TRPA1 (0.5 ng) plus humanTGR5 (2 ng). The cRNAs were dissolved in RNase-free water and the total volume injected was 46 nl. Injected oocytes were stored at 19°C in ND9 solution (mM: N-methyl-D-glucamine-Cl 87, NaCl 9, KCl 2, CaCl_2 1.8, MgCl_2 1, HEPES 5, pH 7.4 with Tris) supplemented with 100 units. ml^{-1} penicillin and 100 $\mu\text{g}.\text{ml}^{-1}$ streptomycin. Oocytes were studied two days after injection using the two-electrode voltage-clamp technique¹⁴. Individual oocytes were superfused with ND96 solution (mM: NaCl 96, KCl 2, CaCl_2 1.8, MgCl_2 1, HEPES 5, pH 7.4 with Tris) at a rate of 2-3 ml/min at room temperature. The TRPA1 activator AITC (50 μ M) and antagonist HC-030031 (15 μ M) were used to activate and inhibit TRPA1 currents, respectively. DCA (500 μ M) was used to activate TGR5. Oocytes were clamped at a holding potential of -60 mV.

Neuropeptide release. Slices (0.4 mm) of rat spinal cord with attached dorsal roots (combined cervical, thoracic, lumbar-sacral segments) were prepared at 4°C as described¹. Slices (100 mg) were superfused

with Krebs solution (mM: NaCl 119, NaHCO₃ 25, KH₂PO₄ 1.2, MgSO₄ 1.5, CaCl₂ 2.5, KCl 4.7, D-glucose 11; 95% CO₂, 5% O₂, 37°C) containing 0.1% BSA and peptidase inhibitors (1 μM phosphoramidon, 1 μM captopril). Tissues were stabilized for 90 min and then superfusate was sampled at 10 min intervals. After collection of 2 basal samples, slices were stimulated with TLCA (500 μM), AITC (100 μM) or vehicle for 60 min. Some tissues were superfused with the TRPA1 antagonist HC-030031 (50 μM) or vehicle for 20 min before and during the stimulus. At the end of the experiment, tissues were blotted and weighed. Fractions (2 ml) were freeze-dried, reconstituted with assay buffer, and GRP and NPPB release were determined by enzyme immunoassays (Phoenix Pharmaceuticals, Burlingame, CA). Peptide concentrations were calculated as fmol.g⁻¹ tissue wet weight. TLCA, AITC and HC-030031 did not cross-react with GRP and NPPB antisera.

Detection of *c-fos* in spinal neurons. FTL mice were habituated by daily handling for 2-3 weeks prior to experimentation. Mice were sedated (5% isoflurane) and DCA (25 μg, 10 μl, s.c.) or vehicle (0.9% NaCl) was injected into the nape of the neck. Other groups of mice were pretreated with the TRPA1 antagonist HC-030031 (100 mg.kg⁻¹) or vehicle by gavage (100 μl) 30 min before DCA injection. At 60 min after DCA injection, mice were anesthetized with isoflurane and transcardially perfused with 20 ml PBS and then 20 ml 4% PFA in PBS. The spinal cord was removed, fixed in 4% PFA (2 h, 4°C), and cryoprotected in 30% sucrose PBS (24 h, 4°C). The cervical spinal cord was frozen in OCT and 30 μm frozen sections were floated in 48 well plates in PBS. Sections were washed (PBS, 2 x 10 min) and incubated in 200 μl of β-galactosidase reaction buffer (1 mg/ml 5-bromo-4-chloro-3-indolyl-β-D-galactopyranoside in PBS, 20 mM MgCl₂, 10 mM potassium ferrocyanide, 10 mM potassium ferrocyanide, 24 h room temperature). The reaction was stopped with 200 μl of formalin. Sections were washed (PBS, 3 x 10 min), mounted onto slides and rinsed with dH₂O. Sections were dehydrated in 50%, 70%, and 100% EtOH, washed in xylene and mounted in DPX mounting medium (Electron Microscopy Sciences, Hatfield, PA, USA). Sections were observed with the ScanScope XT (Aperio, Vista, CA, USA). β-galactosidase- (*c-fos*-) positive cells in the dorsal horn laminae I-III were counted by an observer unaware of the treatment.

Scratching behavior. C57BL/6J, *trpa1*^{-/-} or *trpv1*^{-/-} mice were removed from their home cage at 8 am and placed in individual cylinders on a plastic platform. Animals were acclimated to the experimental room, restraint apparatus and investigator for 2 h periods on three successive days before experiments. To evaluate the pruritogenic effects of DCA, mice were sedated (5% isoflurane) and DCA (25 μg, 10 μl, s.c.) was injected into the nape of the neck. To evaluate the contributions of TRP channels, mice were pretreated with the TRPA1 antagonist HC-030031 (100 mg.kg⁻¹, p.o., in 2% DMSO, 20% cyclodextrin), the TRPV1 antagonist AMG-9810 (40 mg.kg⁻¹, i.p., in 0.9% saline) or vehicle (100 μl) 30 min before DCA injection. Scratching behavior was recorded for 60 min after DCA injection. One scratch is defined as lifting of a hind limb to the nape of the neck and withdrawal from this site, regardless of the number of

strokes. Scratching was recorded by observers blinded to the experimental protocol. Scratching behavior was assessed at ~10 am, 2 h after removing mice from their home cage and withdrawal of food.

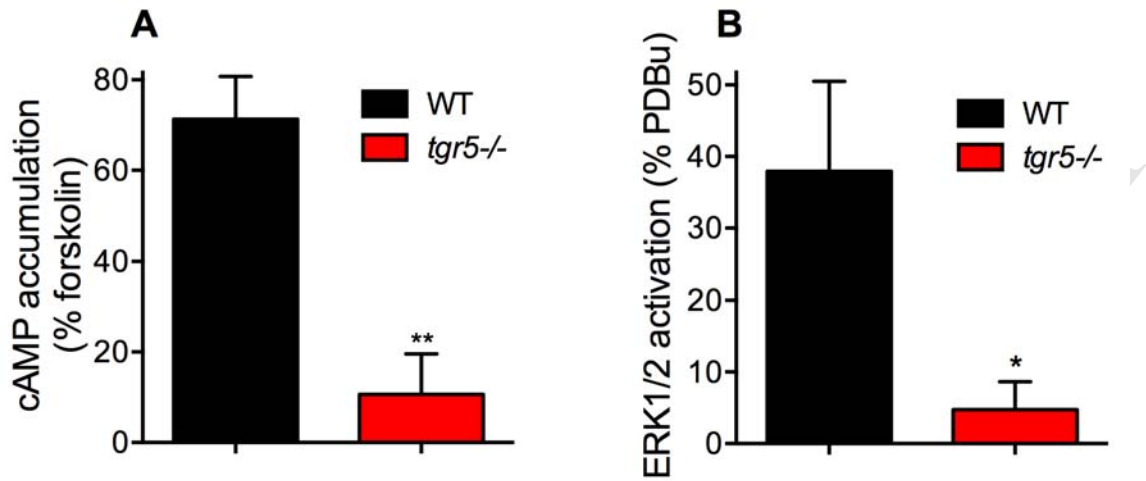
Wiping behavior. The effectiveness of AMG-9810 as a TRPV1 antagonist was assessed by studying capsaicin-evoked wiping behavior¹⁵. Acclimatized C57BL/6J mice received AMG-9810 (40 mg.kg⁻¹, i.p., in 0.9% saline) or vehicle (100 µl) 30 min before injection of capsaicin (3 µg, 10 µl, s.c.) into the cheek. Wiping behavior was recorded at baseline and for 20 min after capsaicin injection by observers blinded to the experimental protocol. A wipe was defined as a singular motion of the ipsilateral (but not bilateral) forelimb beginning at the caudal extent of the injected cheek and proceeding in a rostral direction.

Treatment of *tgr5-tg* mice with BA sequestrant and TGR5 antagonist. To determine the role of endogenous BAs to exacerbated spontaneous scratching, *tgr5-tg* mice were treated with the BA sequestrant colestipol hydrochloride (2.5 mg.kg⁻¹, p.o., Pfizer, Groton, CT) or vehicle (0.9% NaCl, p.o.), which were administered by gavage (100 µl) at 08:00 and 14:00 h for five consecutive days. During this treatment period, mice were habituated as described. After the final gavage treatment, spontaneous scratching behavior was recorded for 60 min. To determine the contribution of TRPA1 to exacerbated spontaneous scratching, *tgr5-tg* mice were treated with HC-030031 (100 mg.kg⁻¹) or vehicle 30 min before scratching behavior was recorded.

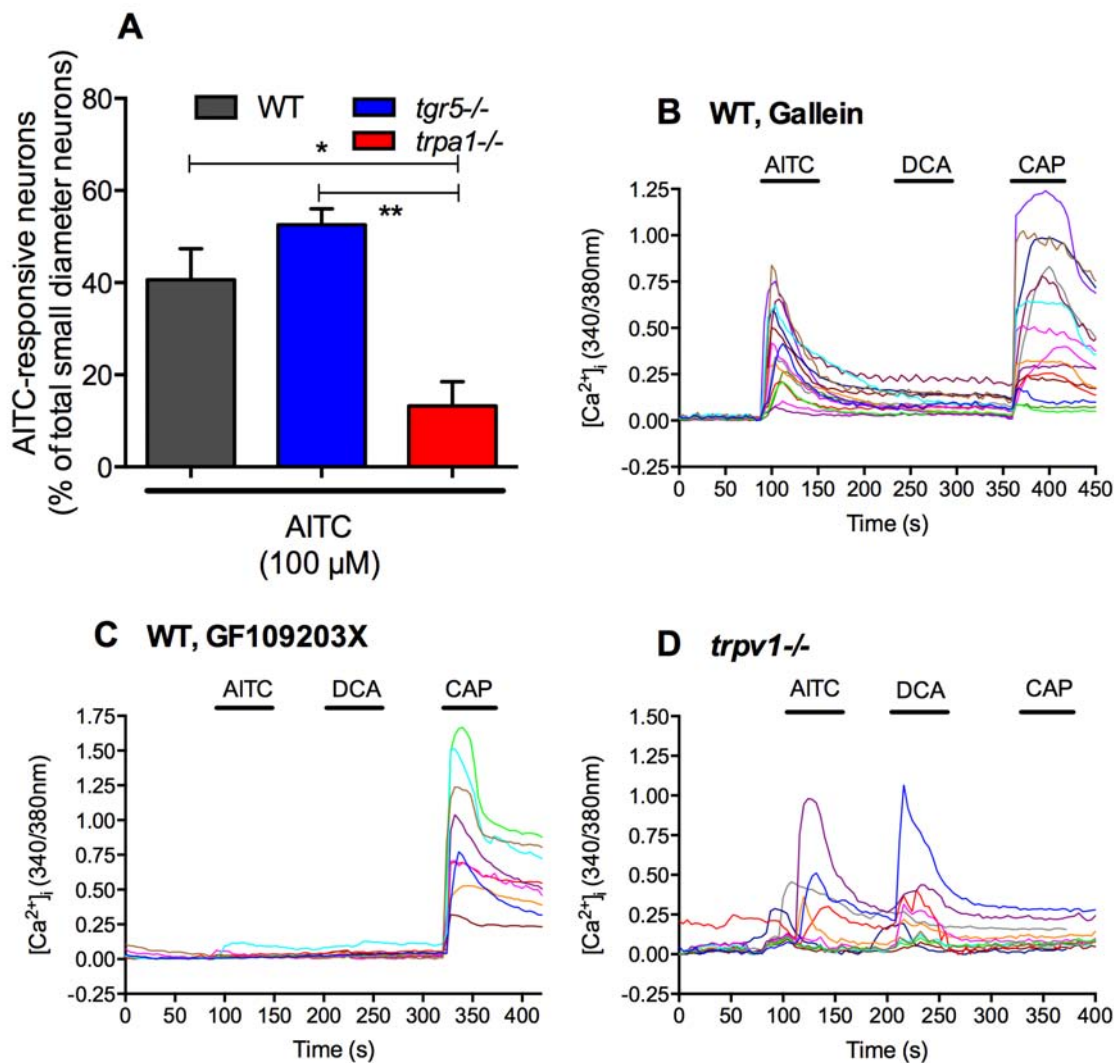
Measurement of plasma BAs. *Tgr5-tg* mice treated with colestipol or vehicle were killed at the end of the scratching assays, ~4 h after food withdrawal. Blood was collected by cardiac puncture into Minicollect tubes (BD Bioscience, North Ryde, Australia) containing sodium EDTA, and plasma was immediately separated by centrifugation (5,000 g, 10 min, 4°C). Total BAs were measured using a Mouse Total BAs kit according to manufacturer's protocol (Crystal Chem, Downers Grove, IL) based on 540 nm absorbance of enzymatic property of 3- α -hydroxy-steroid dehydrogenase.

Statistical analyses. Results are expressed as mean \pm SEM. Data were compared statistically using Graphpad Prism 6, with Student's t-test for comparisons of 2 groups and ANOVA and Bonferroni or Tukey-Kramer *post hoc* test comparisons of multiple groups. A *P*-value less than 0.05 was considered significant.

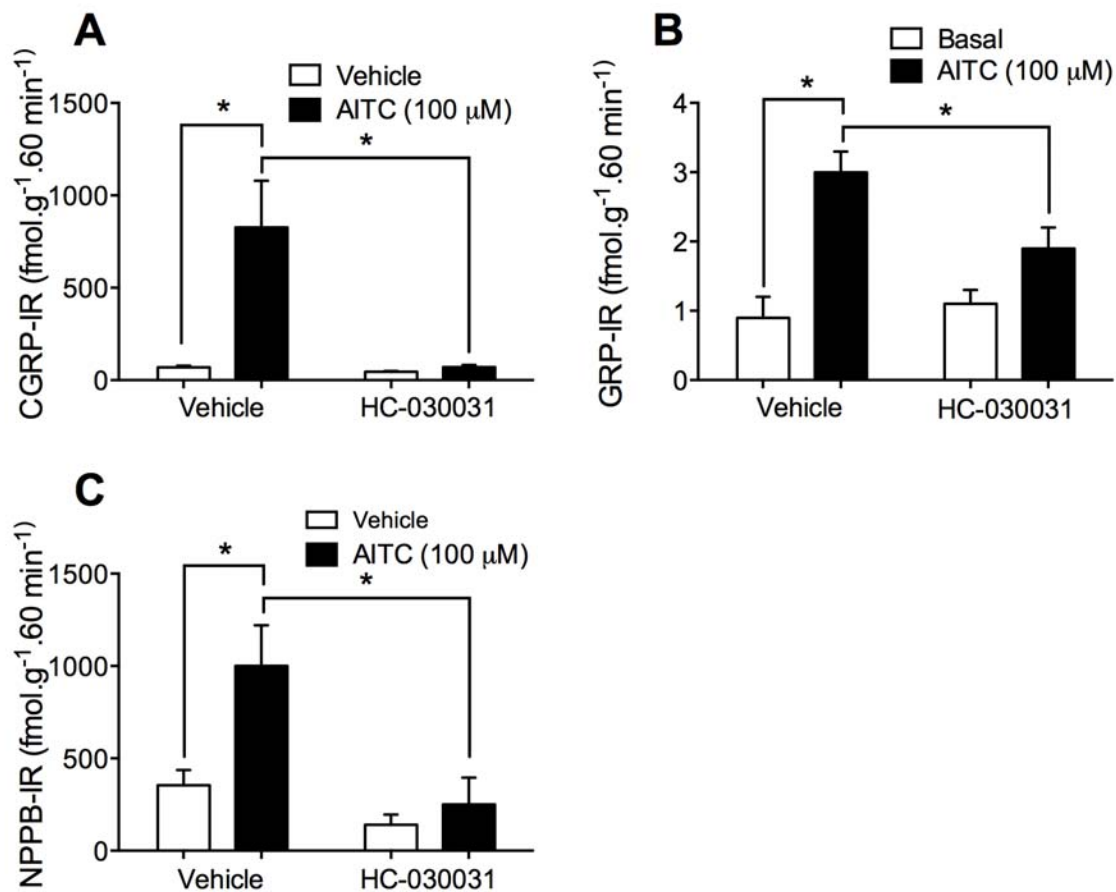
Supplemental Figures



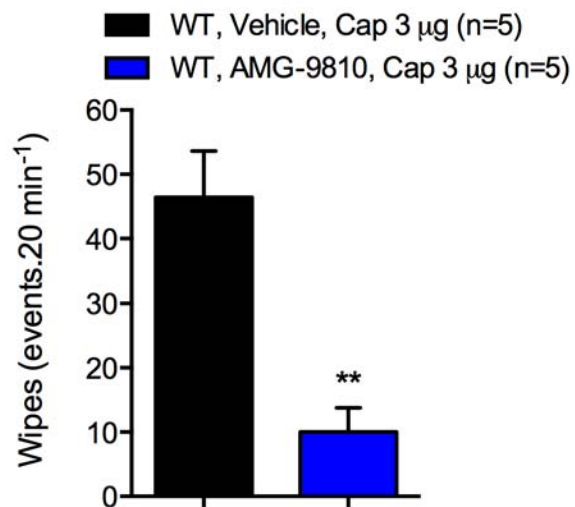
Supplemental Figure 1. TGR5-dependent BA signaling in DRG neurons. A, B. DRG neurons from wild-type (WT) and *tgr5*^{-/-} mice were incubated with DCA (100 μ M, 30 min). Generation of cAMP (A) and activation of ERK1/2 (B) were measured. n=3-6 mice. * P <0.05, ** P <0.01 to WT mice.



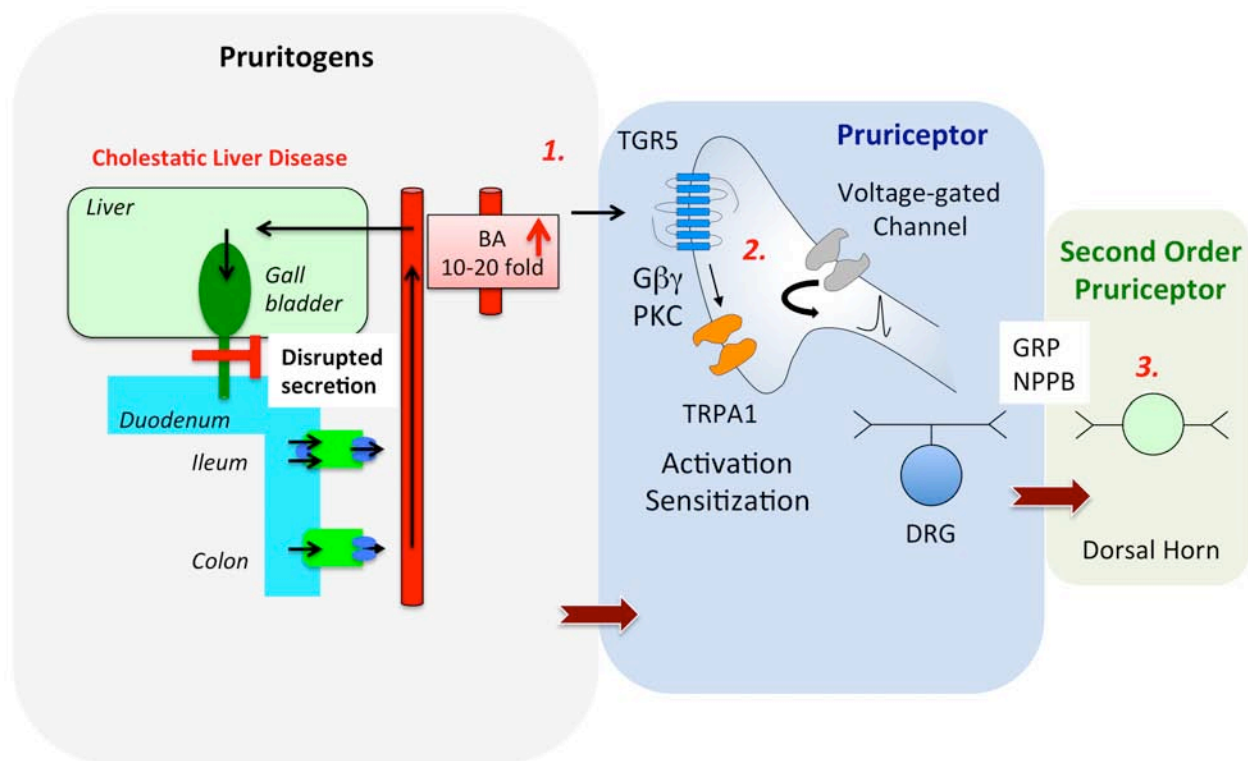
Supplemental Figure 2. G $\beta\gamma$ - and PKC-dependent, but *trpv1*-independent, BA signaling in DRG neurons. [Ca^{2+}]_i was measured in small diameter neurons from WT mice, *tgr5*^{-/-} mice, *trpa1*^{-/-} mice and *trpv1*^{-/-} mice challenged sequentially with AITC (100 μM), DCA (100 μM) and capsaicin (CAP, 1 μM). Responses of KCl (50 mM) -responsive neurons are shown. **A.** Pooled data showing the proportion of AITC-responsive neurons in different experimental groups (2453 neurons, n=22 mice). ** $P < 0.01$, * $P < 0.05$ to AITC in WT or *tgr5*^{-/-}. **B.** WT mice treated with the G $\beta\gamma$ inhibitor gallein. **C.** WT mice treated with the PKC inhibitor GF109203X. **D.** *trpv1*^{-/-} mice. In **B-D**, each line represents a single neuron.



Supplemental Figure 3. AITC-evoked release of neuropeptides. Release of CGRP-IR (A), GPR-IR (B) and NPPB-IR (C) from superfused slices of rat spinal cord treated with vehicle or the TRPA1 agonist AITC (100 μM, 60 min). Tissues were preincubated with vehicle or HC-030031 (50 μM). n=4, **P*<0.05.



Supplemental Figure 4. Antagonism of capsaicin-evoked wiping. Capsaicin was injected into one cheek of wild-type (WT) mice pretreated with the TRPV1 antagonist AMG-9810 or vehicle. Wiping behavior was recorded for 20 min. n=5 mice, **** P <0.01**.



Supplemental Figure 5. Hypothesized model for detection and transmission of BA-evoked itch. 1. Cholestatic liver diseases can induce increased circulating and tissue levels of BAs. **2.** BAs activate TGR5 on first order pruriceptors. TGR5 couples to Gβγ and PKC, which activate and sensitize TRPA1, leading to influx of extracellular Ca²⁺ ions. Activation of voltage sensitive channels results in central transmission to the dorsal horn of the spinal cord. **3.** GRP and NPPB, released within the dorsal horn, excite second order spinal pruriceptors, which transmit pruritogenic signals to higher centers.

Supplemental References

1. Amadesi S, Nie J, Vergnolle N, et al. Protease-activated receptor 2 sensitizes the capsaicin receptor transient receptor potential vanilloid receptor 1 to induce hyperalgesia. *J Neurosci* 2004;24:4300-4312.
2. Kwan KY, Allchorne AJ, Vollrath MA, et al. TRPA1 contributes to cold, mechanical, and chemical nociception but is not essential for hair-cell transduction. *Neuron* 2006;50:277-289.
3. Thomas C, Gioiello A, Noriega L, et al. TGR5-mediated bile acid sensing controls glucose homeostasis. *Cell Metab* 2009;10:167-177.
4. Wilson Y, Nag N, Davern P, et al. Visualization of functionally activated circuitry in the brain. *Proc Natl Acad Sci USA* 2002;99:3252-3257.
5. Bellono NW, Kammel LG, Zimmerman AL, et al. UV light phototransduction activates transient receptor potential A1 ion channels in human melanocytes. *Proc Natl Acad Sci USA* 2013;110:2383-2388.
6. Grant AD, Cottrell GS, Amadesi S, et al. Protease-activated receptor 2 sensitizes the transient receptor potential vanilloid 4 ion channel to cause mechanical hyperalgesia in mice. *J Physiol* 2007;578:715-733.
7. Wilson SR, Gerhold KA, Bifolck-Fisher A, et al. TRPA1 is required for histamine-independent, Mas-related G protein-coupled receptor-mediated itch. *Nat Neurosci* 2011;14:595-602.
8. Poole DP, Godfrey C, Cattaruzza F, et al. Expression and function of the bile acid receptor GpBAR1 (TGR5) in the murine enteric nervous system. *Neurogastroenterol Motil* 2010;22:814-825, e227-818.
9. Cho HJ, Callaghan B, Bron R, et al. Identification of enteroendocrine cells that express TRPA1 channels in the mouse intestine. *Cell Tiss Res* 2014;356:77-82.
10. Bron R, Wood RJ, Brock JA, et al. Piezo2 expression in corneal afferent neurons. *J Comp Neurol* 2014;522:2967-2979.
11. Needham K, Bron R, Hunne B, et al. Identification of subunits of voltage-gated calcium channels and actions of pregabalin on intrinsic primary afferent neurons in the guinea-pig ileum. *Neurogastroenterol Motil* 2010;22:e301-308.
12. **Alemi F, Kwon E**, Poole DP, et al. The TGR5 receptor mediates bile acid-induced itch and analgesia. *J Clin Invest* 2013;123:1513-1530.
13. Lieu T, Udem BJ. Neuroplasticity in vagal afferent neurons involved in cough. *Pul Pharm Therap* 2011;24:276-279.
14. Haerteis S, Krappitz M, Diakov A, et al. Plasmin and chymotrypsin have distinct preferences for channel activating cleavage sites in the gamma subunit of the human epithelial sodium channel. *J Gen Physiol* 2012;140:375-389.
15. Shimada SG, LaMotte RH. Behavioral differentiation between itch and pain in mouse. *Pain* 2008;139:681-687.

Author names in bold designate shared co-first authors